https://doi.org/10.5194/acp-2019-646
Preprint. Discussion started: 4 September 2019

Atmospheric Chemistry and Physics
Discussions

Understanding Climate-Fire-Ecosystem Interactions Using CESM-RESFire and Implications for Decadal Climate Variability

Yufei Zou[1†], Yuhang Wang[1], Yun Qian[2], Hanqin Tian[3], Jia Yang[4], Ernesto Alvarado[5]

[1]School of Earth and Atmospheric Sciences, Georgia Institute of Technology, Atlanta, GA 30332, USA.
[2]Pacific Northwest National Laboratory, Richland, WA 99354, USA.
[3]International Centre for Climate and Global Change Research, School of Forestry and Wildlife Sciences, Auburn University, AL 36849, USA.
[4]College of Forest Resources/Forest and Wildlife Research Center, Mississippi State University, MS 39762, USA.
[5]School of Environmental and Forest Sciences, University of Washington, Seattle, WA 98195, USA.
†Now at Pacific Northwest National Laboratory, Richland, WA 99354, USA.

Correspondence to: Yuhang Wang (yuhang.wang@eas.gatech.edu) and Yufei Zou (yufeizou@gmail.com)

Abstract. Large wildfires exert strong disturbance to regional and global climate systems and ecosystems by perturbing radiative forcing as well as carbon and water balance between the atmosphere and land surface, while short- and long-term variations in fire weather, terrestrial ecosystems, and human activity modulate fire intensity and reshape fire regimes. The complex climate-fire-ecosystem interactions were not included in previous climate model studies, and the resulting effects on the projections of future climate change are not well understood. Here we used a fully interactive REgion-Specific ecosystem feedback Fire model (RESFire) that was developed in the Community Earth System Model (CESM) to investigate these interactions and their impacts on climate systems and fire activity. We designed two sets of decadal simulations using CESM-RESFire for present-day (2001-2010) and future (2051-2060) scenarios, respectively and conducted a series of sensitivity experiments to assess the effects of individual feedback pathways among climate, fire, and ecosystems. Our implementation of RESFire, which includes online land-atmosphere coupling of fire emissions and fire-induced land cover change (LCC), reproduced the observed Aerosol Optical Depth (AOD) from space-based Moderate Resolution Imaging Spectroradiometer (MODIS) satellite products and ground-based AErosol RObotic NETwork (AERONET) data and agreed well with carbon budget benchmarks from previous studies. We estimated the global averaged net radiative effect of both fire aerosols and fire-induced LCC at -0.59 ± 0.52 W m^{-2}, which was dominated by fire aerosol-cloud interactions (-0.82 ± 0.19 W m^{-2}), in the present-day scenario under climatological conditions of the 2000s. The fire-related net cooling effect increased by ~170% to -1.60 ± 0.27 W m^{-2} in the 2050s under the conditions of the Representative Concentration Pathway 4.5 (RCP4.5) scenario. Such greatly enhanced radiative effect was attributed to the largely increased global burned area (+19%) and fire carbon emissions (+100%) from the 2000s to the 2050s driven by climate change. The net ecosystem exchange (NEE) of carbon between the land and atmosphere components in the simulations increased by 33% accordingly, implying that biomass burning is an increasing carbon source at short-term timescales in the future. High-latitude regions with prevalent peatlands would be more vulnerable to increased fire threats due to climate change and

https://doi.org/10.5194/acp-2019-646
Preprint. Discussion started: 4 September 2019

Atmospheric Chemistry and Physics
Discussions

the increase of fire aerosols could counter the climate effects of the projected decrease of anthropogenic aerosols due to air pollution control policies in many regions. We also evaluated two distinct feedback mechanisms that were associated with fire aerosols and fire-induced LCC. On a global scale, the first mechanism imposed positive feedback to fire activity through enhanced droughts with suppressed precipitation by fire aerosol-cloud interactions, while the second one manifested negative feedback due to reduced fuel loads by fire consumption and post-fire tree mortality and recovery processes. These two feedback pathways with opposite effects competed at regional to global scales and increased the complexity of climate-fire-ecosystem interactions and their climatic impacts.

1 Introduction

Large wildfires show profound impacts on human society and the environment with increasing trends in many regions around the world during recent decades (Abatzoglou and Williams, 2016;Barbero et al., 2015;Clarke et al., 2013;Dennison et al., 2014;Jolly et al., 2015;Westerling et al., 2006;Yang et al., 2011;Yang et al., 2015). They pose a great threat to the safety of communities in the vicinity of fire-prone regions and distant downstream areas by both destructive burning and increased health risks from fire smoke exposure. The global annual averaged premature deaths due to fire smoke exposure was estimated at about 339,000 (interquartile range: 260,000-600,000) during 1997 to 2006 (Johnston et al., 2012), while the total cost of fire-related socioeconomic burden would surge much higher if other societal and environmental outcomes, such as morbidity of respiratory and cardiovascular diseases, expenditures of defensive actions and disutility, and ecosystem service damages, were taken into account (Fann et al., 2018;Hall, 2014;Richardson et al., 2012;Thomas et al., 2017). In addition to hazardous impacts on human society, fire also exerts strong disturbance to regional and global climate systems and ecosystems by perturbing radiation budget and carbon balance between the atmosphere and land surface. In return, these short-term and long-term changes in fire weather, terrestrial ecosystems, and human activity modulate fire intensity and reshape fire regimes in many climate change sensitive regions. These complex climate-fire-ecosystem interactions are further confounded by natural processes and human interferences. These processes were not included in previous climate model studies, increasing uncertainties in the projections of future climate variability and fire activity (Flannigan et al., 2009;Hantson et al., 2016;Harris et al., 2016;Liu et al., 2018). Most fire-related climate studies used a one-way perturbation approach by examining a unidirectional forcing and response between climate change and fire activity without feedback. For instance, many historical and future-projected fire responses to climate drivers were mainly based on offline statistical regression or one-way coupled prognostic fire models in earth system models, while fire feedback to weather, climate, and vegetation was neglected (e.g., Abatzoglou et al., 2019;Flannigan et al., 2013;Hurteau et al., 2014;Liu et al., 2010;Moritz et al., 2012;Parks et al., 2016;Wotton et al., 2017;Young et al., 2017;Yue et al., 2013). The neglected feedback could affect regional to global radiative forcing, biogeochemical and hydrological cycles, and ecological functioning that may in turn modulate fire activity in local and remote regions (Harris et al., 2016;Liu, 2018;Pellegrini et al., 2018;Seidl et al., 2017;Shuman et al., 2017). Similarly, climate studies (e.g., Jiang et al., 2016;Tosca et al., 2013;Ward et al., 2012) that focused on climate responses to fire forcing used the same approach but from an opposite perspective, in which they evaluated multiple fire impacts on climate systems through fire aerosols, greenhouse gases, and land albedo effects using climate sensitivity experiments with and without fixed fire emissions as model inputs.

However, possible fire activity and emission changes in response to these fire weather and climate variations were missing in such one-way perturbation modeling approaches.

To tackle these problems, we developed a two-way coupled RESFire model (Zou et al., 2019) with online land-atmosphere coupling of fire-related mass and energy fluxes as well as fire-induced land cover change in CESM (hereafter as CESM-RESFire). CESM-RESFire performed well using either offline observation-/reanalysis-based atmosphere data or online simulated atmosphere, which were applied in this study to investigate the complex climate-fire-ecosystem interactions as well as to project future climate change with fully interactive fire disturbance. In this work, we used the state-of-the-science CESM-RESFire model to evaluate major feedback in climate-fire-ecosystem interactions through biogeochemical, biogeophysical, and hydrological pathways and to assess future changes of decadal climate variability and fire activity with consideration of these interactive feedback processes. We provided a brief model description and sensitivity experiment settings in Section 2 and presented modeling results and analyses on radiative effects, carbon balance, and feedback evaluation in Section 3. Final conclusions and implications followed in Section 4.

2 CESM-RESFire description, simulation setup, and benchmark data

2.1 Fire model and sensitivity simulation experiments

RESFire (Zou et al., 2019) is a process-based fire model developed in the CESM version 1.2 modeling framework that incorporates ecoregion-specific natural and anthropogenic constraints on fire occurrence, fire spread, and fire impacts in both the CESM land component—the Community Land Model version 4.5 (CLM4.5) (Oleson et al., 2013) and the atmosphere component—the Community Atmosphere Model version 5.3 (CAM5) (Neale et al., 2013). It is compatible with either observation/reanalysis-based data atmosphere or the CAM5 atmosphere model with online land-atmosphere coupling through aerosol-climate effects and fire-vegetation interactions. It includes two major fire feedback pathways: the atmosphere-centric fire feedback through fire-related mass and energy fluxes and the vegetation-centric fire feedback through fire-induced land cover change. These feedback pathways correspond to two key climate variables, radiative forcing and carbon balance, through which fires exert their major climatic and ecological impacts. Other features in CLM4.5 and CAM5, such as the photosynthesis scheme (Sun et al., 2012), the MAM3 aerosol module (Liu et al., 2012), and the cloud macrophysics scheme (Park et al., 2014), allow for more comprehensive assessments of climate effects of fires through the interactions with vegetation and clouds. We also implemented distribution mapping-based online bias corrections for key fire weather variables (i.e., surface temperature, precipitation, and relative humidity) to reduce negative influences of climate model biases in atmosphere simulation and projection. Please refer to Zou et al. (2019) for more detailed fire model descriptions and to Sofiev et al. (2012) for the fire plume rise parameterization. A new fire plume rise scheme (Ke et al., 2019) is under development and will be implemented in CESM-RESFire in the future. To quantify the impacts of fire-climate interactions under different climatic conditions, we designed two groups of sensitivity simulations for present-day and future scenarios (Table 1). In each simulation group, we conducted one control run (CTRLx, where x=1 or 2 indicates the present-day or future scenario, respectively) and two sensitivity runs (SENSxA/B, where x is the same as that in CTRL runs and the notations of A and B are explained below). The CTRL runs were designed with fully interactive fire disturbance

https://doi.org/10.5194/acp-2019-646
Preprint. Discussion started: 4 September 2019

Atmospheric Chemistry and Physics Discussions

such as fire emissions with plume rise and fire-induced LCC with different boundary conditions for a present-day scenario (CTRL1) and a moderate future emission scenario (CTRL2) of the Representative Concentration Pathway 4.5 (RCP4.5), respectively. In each scenario, we turned off the atmosphere-centric feedback mechanisms (e.g., fire aerosol climate effects) in SENSxA simulations (where x=1 or 2) and then turned off both atmospheric-centric and vegetation-centric fire feedback (e.g., fire-induced LCC) in SENSxB simulations. Consequently, we estimated the atmosphere-centric impacts of fire emissions on radiative forcing in the present-day scenario (RCP4.5 future scenario) by comparing SENS1A (SENS2A) with CTRL1 (CTRL2). We also estimated the vegetation-centric impacts of fire-induced LCC on terrestrial carbon balance in the present-day scenario (RCP4.5 future scenario) by comparing SENS1B (SENS2B) with SENS1A (SENS2A). The net fire-related effects were evaluated by comparing CTRL runs with SENSxB runs as both fire feedback mechanisms were turned off in the SENSxB runs. Using these sensitivity experiments, we evaluated two-way climate-fire-ecosystem interactions under the same integrated modeling framework that was not possible in one-way perturbation studies considering either climate impacts on fires (Kloster et al., 2010;Kloster et al., 2012;Thonicke et al., 2010) or fire feedback to climate (Jiang et al., 2016;Li et al., 2014;Ward et al., 2012;Yue et al., 2015;Yue et al., 2016).

2.2 Model input data

We used the spun-up files from previous long-term runs (Zou et al., 2019) as initial conditions for the present-day experiments (CTRL1 and SENS1A/B). The boundary conditions including the prescribed climatological (1981-2010 average) sea surface temperature and sea ice data for the present-day scenario were obtained from the Met Office Hadley Centre (HadISST) (Rayner et al., 2003). Similarly, the nitrogen and aerosol deposition rates were also prescribed from a time-invariant spatially varying annual mean file for 2000 and a time-varying (monthly cycle) globally-gridded deposition file, respectively, as the standard datasets necessary for the present-day CAM5 simulations (Hurrell et al., 2013). The climatological 3-hourly cloud-to-ground lightning data via bilinear interpolation from NASA LIS/OTD grid product v2.2 (http://ghrc.msfc.nasa.gov) 2-hourly lightning frequency data and the world population density data were fixed at the 2000 levels for all the present-day simulations. The non-fire emissions from anthropogenic sources (e.g., industrial, domestic and agriculture activity sectors) in the present-day scenario were from the emission dataset (Lamarque et al., 2010) in the year 2000 for the Fifth Assessment Report of the Intergovernmental Panel on Climate Change (IPCC AR5). We replaced the old prescribed GFED2 fire emissions (van der Werf et al., 2006) in the default offline emission data with online coupled fire emissions generated by the RESFire model in the CTRL runs. We then decoupled online simulated fire emissions in the SENS1A runs, in which fire emissions were not transported to the CAM5 atmosphere model, to isolate the atmosphere-centric impacts of fire-climate interactions. In both CTRL1 and SENS1A experiments, we perturbed the semi-static historical LCC data for the year 2000 from the version 1 of the Land-Use History A product (LUHa.v1) (Hurtt et al., 2006) through post-fire vegetation changes (Zou et al., 2019). We then used the fixed LCC data for the year 2000 in the SENS1B run and compared two SENS1 runs (SENS1A-SENS1B) to evaluate the vegetation-centric fire impacts on terrestrial ecosystems and carbon balance in the 2000s.

https://doi.org/10.5194/acp-2019-646
Preprint. Discussion started: 4 September 2019

Atmospheric Chemistry and Physics Discussions

For the future scenario experiments, we replaced all the present-day datasets with the RCP4.5 projection datasets including the initial conditions and prescribed boundary conditions of global SST and sea ice data in 2050, the cyclical non-fire emissions and deposition rates fixed in 2050 under the RCP4.5 scenario, and the annual LCC data for the RCP4.5 transient period in 2050 based on the Future Land-Use Harmonization A products (LUHa.v1_future) (Hurtt et al., 2006). All these datasets were described in the technical note of CAM5 (Neale et al., 2013) and stored on the Cheyenne computing system (CISL, 2017) at the National Center for Atmospheric Research (NCAR)-Wyoming Supercomputing Center (NWSC). It is worth noting that we used the same population density data and climatological lightning data in the future scenario with the present-day scenario given great uncertainties in future projections of these inputs. In other words, we did not consider the influence of demographic changes or lightning frequency changes in our future projection simulations but focused on broad impacts of future climate change on fuel loads and fire weather except lightning.

The global mean GHG mixing ratios in the CAM5 atmosphere model were fixed at the 2000-year levels (CO_2: 367.0 ppmv; CH_4:1760.0 ppbv; N_2O:316.0 ppbv) in all present-day experiments and they were replaced by the prescribed RCP4.5 projection datasets with the well-mixed assumption and monthly variations in the future scenarios. These GHG mixing ratios were then passed to the CLM4.5 land model in all sensitivity experiments. In return, the land model provided the diagnostics of the balance of all carbon fluxes between net ecosystem production (NEP, g C m^{-2} s^{-1}, positive for carbon sink) and depletion from fire emissions, landcover change fluxes, and carbon loss from wood products pools, and then the computed net CO_2 flux was passed to the atmosphere model in forms of net ecosystem exchange (NEE, g C m^{-2} s^{-1}). Though fire emissions could perturb the value of NEE at short-term scales, it is often assumed that fire is neither a source nor a sink for CO_2 since fire carbon emissions are offset by carbon absorption of vegetation regrowth over long-term scales (Bowman et al., 2009). Therefore, we did not consider the radiative effect of fire-related greenhouse gases (GHGs) in our sensitivity experiments. This kind of "concentration-driven" simulations with prescribed atmospheric CO_2 concentrations for a given scenario have been used extensively in previous fire-climate interaction assessments (e.g., Kloster et al., 2010;Li et al., 2014; Thonicke et al., 2010) and most of the RCP simulations (Ciais et al., 2013).

2.3 Model evaluation benchmarks and datasets

Multiple observational and assimilated datasets were applied to evaluate the modeling performance regarding radiative forcing. We collected space-based column aerosol optical depth (AOD) from the level-3 MODIS Aqua monthly global product (MYD08_M3, Platnick et al., 2015) and ground-based version 3 aerosol optical thickness (AOT) level 2.0 data from the Aerosol Robotic Network (AERONET, https://aeronet.gsfc.nasa.gov/) project for comparison with the model simulated AOD data at 550 nm. The AERONET AOT at 550 nm were interpolated by estimating Ångström exponents based on the measurements taken at two closest wavelengths at 500 nm and 675 nm (see supplement for details). We then followed the Ghan's method (Ghan, 2013) to estimate fire aerosol radiative effects (RE_{aer}) on the planetary energy balance in terms of aerosol-radiation interactions (RE_{ari}), aerosol-cloud interactions (RE_{aci}), and fire aerosol-related surface albedo change (RE_{sac}) in Eq. (1). The radiative effect related to fire-induced land cover change (RE_{lcc}) was estimated by comparing shortwave radiative fluxes at the top-of-atmosphere (TOA) between SENSxA

https://doi.org/10.5194/acp-2019-646
Preprint. Discussion started: 4 September 2019

Atmospheric Chemistry and Physics
Discussions

(with fire-induced LCC) and SENSxB (without fire-induced LCC) experiments. By summing up all these terms, we estimated the fire-related net radiative effect (RE_{fire}) as the shortwave radiative flux difference between CTRLx (with fire aerosols and fire-induced LCC) and SENSxB (without fire aerosols and fire-induced LCC) experiments:

$$\begin{gathered} fire\ aerosol - radiation\ interaction\ RE{:}\ RE_{ari} = \Delta(F - F_{clean}) \\ fire\ aerosol - cloud\ interaction\ RE{:}\ RE_{aci} = \Delta\left(F_{clean} - F_{clear,clean}\right) \\ fire\ aerosol - related\ surface\ albedo\ change\ RE{:}\ RE_{sac} = \Delta F_{clear,clean} \\ fire\ aerosol\ net\ RE{:}\ RE_{aer} = RE_{ari} + RE_{aci} + RE_{sac} = F_{CTRLx} - F_{SENSxA} \\ fire - induced\ land\ cover\ change\ RE{:}\ RE_{lcc} = F_{SENSxA} - F_{SENSxB} \\ fire - related\ net\ RE{:}\ RE_{fire} = RE_{aer} + RE_{lcc} = F_{CTRLx} - F_{SENSxB} \end{gathered}, \quad (1)$$

where Δ is the difference between control and sensitivity simulations, F is the shortwave radiative flux at the TOA, F_{clean} is the radiative flux calculated as an additional diagnostics from the same simulations but neglecting the scattering and absorption of solar radiation by all aerosols, and $F_{clear,clean}$ is the flux calculated as additional diagnostic but neglecting scattering and absorption by both clouds and aerosols. The surface albedo effect is largely the contribution of changes in surface albedo induced by fire aerosol deposition and land cover change, which is small but nonnegligible in some regions (Ghan, 2013). We used similar modeling settings including the 3-mode modal aerosol scheme (MAM3) (Liu et al., 2012) and the Snow, Ice, and Aerosol Radiative (SNICAR) module (Flanner and Zender, 2005) and compared our online coupled fire modeling results against previous offline prescribed fire modeling studies (Jiang et al., 2016;Ward et al., 2012) in the next section.

We also examined the modeling performance on burned areas and terrestrial carbon balance such as fire carbon emissions, gross primary production (GPP, g C m^{-2} s^{-1}, positive for vegetation carbon uptake), net primary production (NPP, g C m^{-2} s^{-1}, positive for vegetation carbon uptake), net ecosystem productivity (NEP, g C m^{-2} s^{-1}, positive for net ecosystem carbon uptake), and net ecosystem exchange (NEE, g C m^{-2} s^{-1}, positive for net ecosystem carbon emission). The model simulated burned areas and fire carbon emissions were evaluated against the satellite based GFED4.1s datasets (Giglio et al., 2013;Randerson et al., 2012;van der Werf et al., 2017), and these carbon budget related variables were calculated in Eqs. (2) and (3) and compared with the MODIS primary production products (Zhao et al., 2005;Zhao and Running, 2010), previous modeling results used for terrestrial model comparison projects (Piao et al., 2013) and the IPCC AR5 report (Ciais et al., 2013), and the global carbon budge assessment (Le Quere et al., 2013) by the broad carbon cycle science community.

$$\mathrm{GPP} = \mathrm{NPP} + R_a = (\mathrm{NEP} + R_h) + R_a, \quad (2)$$

$$\mathrm{NEE} = C_{fe} + C_{lh} - \mathrm{NEP} = C_{fe} + C_{lh} + R_h + R_a - \mathrm{GPP}, \quad (3)$$

where R_a is the total ecosystem autotrophic respiration (g C m^{-2} s^{-1}), R_h is the total heterotrophic respiration (g C m^{-2} s^{-1}), C_{fe} is the fire carbon emissions (g C m^{-2} s^{-1}), and C_{lh} is the carbon loss (g C m^{-2} s^{-1}) due to land cover change, wood products, and harvest.

3 Modeling results and discussion

3.1 Fire-related radiative effects

We compared the model simulated 10-year annual averaged column AOD at 550nm from CTRL1 and space-based AOD from MODIS aboard the Aqua satellite in Fig. 1. It's noted that both AOD data resulted from all sources

https://doi.org/10.5194/acp-2019-646
Preprint. Discussion started: 4 September 2019

Atmospheric Chemistry and Physics
Discussions

including fire and non-fire emissions, and significant differences existed in specific regions due to large biases in model emission inputs and aerosol parameterization. In the MODIS AOD data, the most noticeable hotspot regions include eastern China, South Asia such as India, and Africa. The first two regions are contributed mostly by anthropogenic emissions, while the last one is dominated by fire emissions. Since the non-fire emissions used in CAM5 simulations were 2000-based (Lamarque et al., 2010) and low biased comparing to rapid emission increases in many Asian developing countries (Kurokawa et al., 2013), the simulated hotspot regions in East and South Asia were not as appreciable as those observed in the remote sensing data. The model results also show underestimation in rainforests over South America and Central Africa, where large fractions of aerosols are contributed by primary and secondary organic aerosols from biogenic sources and precursors (Gilardoni et al., 2011) that were missing in the simulation. However, the model well captured the high AOD regions over the Northern and Southern Hemispheres of Africa with the dominant role of biomass burning emissions in this region. It's also noticeable that the CAM5 model overestimated dust emissions significantly with some spuriously high AOD hotspots emerging over the Sahara, Arabian, South Africa, and Central Australia desert regions. This overestimation problem was also found in previous dust AOD modeling studies (Ridley et al., 2016).

To further evaluate the fire-related AOD modeling performance, we compared the difference between CTRL1 and SENS1A to isolate aerosol contributions from fire sources in Fig. 2. The spatial distribution of fire-related AOD clearly highlighted African savanna as a major biomass burning region. We also compared monthly AOD at six fire-prone regions with AERONET in situ observations to get a better understanding of temporal variations of fire aerosols. Most sites showed strong seasonal variations in monthly AOD as observed by AERONET, and the CESM-RESFire model well captured fire seasonality in these regions. Generally, the model AOD results were at the lower ends of the uncertainty ranges of ground in situ observations in most regions due to limited spatial representativeness of coarse model grid resolution and fire emissions, especially over African savannas like Ilorin (Fig. 2e) and Southeast Asian rainforests like Jambi (Fig. 2g) where agricultural and deforestation related burning activity prevails.

Lastly, we estimated radiative effects of fire aerosols and fire-induced land cover change and compared the results with previous studies in Fig. 3 and Table 2. The radiative effect of fire aerosol-radiation interactions (RE_{ari}) was most prominent in tropical Africa and downwind Atlantic Ocean areas as well as South America and eastern Pacific. High-latitude regions like eastern Siberia also showed significant positive radiative effects due to fire emitted light absorbing aerosols such as black carbon (BC). The land-sea contrast warming and cooling radiative effects over Africa and South America were attributed to differences of cloud cover fractions over land and ocean areas (Jiang et al., 2016). In these regions, cloud fractions and liquid water path are much larger over downwind ocean areas than land areas during the fire season. Cloud reflection of solar radiation strongly enhances light absorption by fire aerosols residing above low-level clouds over ocean areas (Abel et al., 2005;Zhang et al., 2016).

The radiative effect of fire aerosol-cloud interactions (RE_{aci}) showed generally cooling effects in most regions due to scattering and reflections by enhanced cloudiness, and these cooling effects were more pervasive over high-latitude regions such as boreal forests in North America and eastern Siberia. Similar land-sea contrast radiative effects emerged again in the vicinity of Africa and South America, but the signs of the contrast effect related with aerosol-cloud interactions were opposite to these with aerosol-radiation interactions. The radiative effect of fire aerosol-related

https://doi.org/10.5194/acp-2019-646
Preprint. Discussion started: 4 September 2019

surface albedo change (RE_{sac}) showed similarly spatial patterns with moderate cooling effects in boreal regions, which were related to fire aerosol-induced snow precipitation and surface albedo change (Ghan, 2013). Besides spatial heterogeneity in fire-induced radiative effects, these radiative effects also showed significant temporal variations that were related with fire seasonality. Figure 4 shows zonal averaged time-latitude cross sections of fire aerosol emissions and fire-induced changes in clouds and radiative effects. Massive fire carbonaceous emissions shifted from the Northern Hemisphere tropical regions in boreal winter to the Southern Hemisphere tropical regions in boreal summer, when similar amounts of fire emissions were also observed in boreal mid- and high-latitude regions (Fig. 4a/b). Fire aerosols greatly increased cloud condensation nuclei (CCN, Fig. 4c) and cloud droplet number concentrations (CDNUMC, Fig. 4d) in these regions, while the increase in cloud water path (CWP, Fig. 4e) and low cloud fraction (CLDLOW, Fig. 4f) were more significant in boreal high-latitude regions than in the tropics. The low solar zenith angle in high-latitude regions enhanced solar radiation absorption by light-absorbing aerosols and resulted in stronger changes in radiative effects by aerosol-radiation interactions during boreal summer (Fig. 4g). In the meantime, increased CWP and CLDLOW in high-latitude regions also leaded to much stronger cooling effects by aerosol-cloud interactions (RE_{aci}) (Fig. 4h), which overwhelmed the increase in RE_{ari}. These modeling results based on the online coupled RESFire model show similar spatiotemporal patterns with these in Jiang et al. (2016) that were driven by offline prescribed fire emissions.

In general, the 10-year averaged global mean values and standard deviations of interannual variations for fire aerosol-related RE_{ari}, RE_{aci}, and RE_{sac} in the 2000s were -0.003 ± 0.013 W m^{-2}, -0.82 ± 0.19 W m^{-2}, and 0.19 ± 0.61 W m^{-2}, respectively, and fire-induced RE_{lcc} was 0.04 ± 0.38 W m^{-2}. After combining all these forcing terms, we estimated a net RE_{fire} of -0.59 ± 0.51 W m^{-2} for the present-day scenario that is larger than the estimate of -0.55 W m^{-2} in the previous fire radiative effect studies (Jiang et al., 2016;Ward et al., 2012). It is noted that both Ward et al. (2012) and Jiang et al. (2016) used prescribed fire emissions from CLM3 model simulations (Kloster et al., 2010;Kloster et al., 2012) and GFED datasets (Giglio et al., 2013;Randerson et al., 2012), respectively, for their uncoupled fire sensitivity simulations. The annual fire carbon emissions used by Ward et al. (2012) ranged from 1.3 Pg C yr^{-1} for the present-day simulation to 2.4 Pg C yr^{-1} for the future projection with ECHAM atmospheric forcing, while the fire BC, POM and SO_2 emissions used by Jiang et al. (2016) were based on the GFEDv3.1 dataset with an annual averaged fire carbon emission of 1.98 Pg C yr^{-1} (Randerson et al., 2012). Their fire emissions were lower than the RESFire model simulation of 2.6 Pg C yr^{-1} (Table 3) in this study, which might result in the differences in the estimates of fire aerosol radiative effects. It is also worth noting that all fire emissions were released into the lowest CAM level as surface sources by Ward et al. (2012), and a default vertical profile of fire emissions based on the AeroCom protocol (Dentener et al., 2006) was used by Jiang et al. (2016) in their CAM5 simulations. In our simulations, we used a simplified plume rise parameterization (Sofiev et al., 2012) in CESM-RESFire and applied online calculated vertical profiles with diurnal cycles to the vertical distribution of fire emissions. The simulations of annual median heights of fire plumes for the present-day and RCP4.5 future scenarios were shown in Fig. 5. Previous observation-based injection height studies suggested that only 4–12% fire plumes could penetrate planetary boundary layers with most fire plumes stay within the near surface atmosphere layers (val Martin et al., 2010;Ke et al., 2019). Our plume-rise simulation results agreed with these estimates, though a quantitative comparison is beyond the scope

https://doi.org/10.5194/acp-2019-646
Preprint. Discussion started: 4 September 2019

Atmospheric Chemistry and Physics Discussions

of this study because of the inconsistency between simulated and actual meteorological conditions. It is also noted that there was no systematic change in plume rise height distributions between the RCP4.5 future scenario and present-day scenarios, both of which showed most fire plumes (~80%) rise less than 1000 m. Comparing to surface released fire emissions in previous studies (Ward et al., 2012), our higher elevated fire plumes affected the vertical distribution and lifetime of fire aerosols and further influenced regional radiative effects after long-range transport of fire aerosols. Lastly, we compared the future scenario results with the present-day conditions in Table 2, which suggests a 171% increase of net fire aerosol and land cover change radiative effects from -0.59 ± 0.51 W m^{-2} in the present-day scenario to -1.60 ± 0.27 W m^{-2} in the RCP4.5 future scenario. Such enhanced negative radiative forcing is dominated by the increased RE_{aci} of fire aerosol-cloud interactions that is much larger than the CCSM future projection results (+51%) in Ward et al. (2012). It is noted that the net estimate of fire radiative forcing changes in Ward et al. (2012) included other offline-based fire climate effects such as fire-related GHGs impacts and climate-biogeochemical cycle feedback, which could dampen or strengthen the cooling effect of fire aerosols.

3.2 Fire-related disturbance to carbon balance

In addition to the atmosphere-centric fire-induced radiative effects, we also evaluated the vegetation-centric terrestrial carbon budget changes. We used the previous model inter-comparison studies and the latest GFEDv4.1s datasets as evaluation benchmarks and examined fire-related metrics including global burned area and fire carbon emissions (Fig. 6 and Table 3). We also collected global scale GPP, NPP, and NEE from previous literatures (Ciais et al., 2013; Piao et al., 2013;Zhao and Running, 2010) to compare with our simulation results (Table 3). The RESFire model performed well in global burned area and fire carbon emissions driven by either offline observation-/reanalysis-based CRUNCEP atmosphere data (RESFire_CRUNCEP) and online CAM5 simulated atmosphere data after bias corrections (RESFire_CAM5c). The annual averaged burned area results of both RESFire_CRUNCEP (508 ± 15 Mha yr^{-1}) and RESFire_CAM5c (472 ± 14 Mha yr^{-1}) are very close to the GFEDv4.1s benchmark value of 510 ± 27 Mha yr^{-1}, while the default fire model in CLM (322 Mha yr^{-1}) is significantly low biased. For fire carbon emissions, the offline RESFire_CRUNCEP result (2.3 ± 0.2 Pg C yr^{-1}) agrees well with the GFEDv4.1s benchmark of around 2.2 ± 0.4 Pg C yr^{-1}, and the online RESFire_CAM5c result shows a 18% higher value (2.6 ± 0.1 Pg C yr^{-1}) than the benchmark. Since the GFED emission datasets are low biased due to low satellite detection rates for small fires under canopy and clouds, previous fire studies (Johnston et al., 2012;Ward et al., 2012) rescaled fire emissions in their practice for climate and health impact assessment. Here, a moderate increase in online estimated fire carbon emissions would reduce the need for fire emission rescaling. Such difference is also consistent with the changes in different versions of the GFED datasets, which show a 11% increase of global fire carbon emissions in the latest GFED4s as compared with the old GFED3 for the overlapping 1997-2011 time period (van der Werf et al., 2017). Since carbon emissions from deforestation fires and other land use change processes are a key component to estimate global carbon budget (Le Quere et al., 2013), improved fire emission estimation would benefit carbon budget simulation in the land model.

We then compared the CLM simulated carbon budget variables such as GPP and NEE against 10 process-based terrestrial biosphere models that were used for the IPCC fifth Assessment Report (Piao et al., 2013). Both the offline and online CLM GPP results are around 142 Pg C yr^{-1}, which are higher than the MODIS primary production products

(MOD17) of 109.29 Pg C yr^{-1} (Zhao et al., 2005) and near the upper bound of ensemble modeling results (133 $\pm$ 15 Pg C yr^{-1}) (Piao et al., 2013). Such high GPP estimation leads to ~11% higher NPP in the CLM simulations than the MODIS global average annual NPP product of 53.5 Pg C yr^{-1} from 2001 to 2009 (Zhao and Running, 2010) as well as the old modeling result (54 Pg C yr^{-1}) based on the default fire model in CLM developed by Li et al. (2013;2014) (hereafter as CLM-LL2013). These differences may result from the different atmosphere forcing data used to drive the CLM land model. However, the NEE results based on the CESM-RESFire model are consistent with the benchmarks from the IPCC AR5 (Ciais et al., 2013) and ensemble modeling results (Piao et al., 2013), indicating a good land modeling performance with online fire disturbance in CESM.

After the evaluation of carbon budget in the CLM land model, we further decomposed the components in NEE and compared the new CESM-RESFire simulation results with previous fire model simulations by Li et al. (2014). Following their experiment setting in Li et al. (2014), we isolated fire contributions to each carbon budget variables by differencing the fire-on and fire-off experiments driven by the CRUNCEP data atmosphere in Table 4. We found a 58% increase in fire-induced NEE variations simulated by CESM-RESFire than CLM-LL2013. This increase was attributed to enhanced fire emissions and suppressed NEP in CESM-RESFire. As discussed in the previous section, CESM-RESFire simulated higher annual averaged fire carbon emissions (2.08 Pg C yr^{-1}) than CLM-LL2013 (1.9 Pg C yr^{-1}), which contributed 31% of the difference in their NEE changes. Furthermore, CESM-RESFire simulated smaller NEP changes due to fire disturbance, which could be attributable to fire-induced land cover change in RESFire. We considered fire-induced whole plant mortality and post-fire vegetation recovery in the new CESM-RESFire model (Zou et al., 2019), both of which were not included in the default CLM-LL2013 model. The newly incorporated fire-induced land cover change would influence ecosystem productivity and respiration as shown by carbon budget variables in Table 4. Specifically, the fire-induced whole plant mortality and recovery would moderate the variations in ecosystem productivity and respiration and further suppress fire-induced NEP changes. The suppressed NEP change explained 52% of the total difference between CESM-RESFire and CLM-LL2013 in simulated NEE changes.

Similar suppression effects of fires on NEP were also found in Seo and Kim (2019), in which they used the CLM-LL2013 fire model but enabled the dynamic vegetation (DV) mode to simulate post-fire vegetation changes. Though the DV mode of the CLM model is capable of simulating vegetation dynamics, considerable biases exist in the online simulation of land cover change by the coupled CLM-DV model (Quillet et al., 2010) and may undermine the interpretation of fire-related ecological effects. For instance, the global fractions of bare ground and needleleaf trees in the CLM-DV simulations were much larger than these in the non-DV (BGC only) simulation in Seo and Kim (2019), while the fractions of shrub and broadleaf trees with active DV were less than these without DV regardless of whether fire disturbance were included or not in the simulations. These biases could distort ecosystem properties such as primary production and carbon exchange as well as fire-related ecological effects.

Similar to fire-related radiative effects, we examined changes of carbon budget variables in the RCP4.5 future scenario in Table 5 and Fig. 7. The global burned area increased by 19% from the present-day scenario in CTRL1 (464 $\pm$ 19 Mha yr^{-1}) to the RCP4.5 future scenario in CTRL2 (551 $\pm$ 16 Mha yr^{-1}) (Fig. 7a). Accordingly, the annual averaged fire carbon emission increased by 100% from 2.5 $\pm$ 0.1 Pg C yr^{-1} at present to 5.0 $\pm$ 0.3 Pg C yr^{-1} in the future (Fig. 7b). This increase is larger than a previous CLM simulated result of 25%~52% by Kloster et al.

https://doi.org/10.5194/acp-2019-646
Preprint. Discussion started: 4 September 2019

(2010;2012), which might result from different climate sensitivity between CESM-RESFire and CLM-LL2013. It's noted that recent satellite-based studies found decreasing trends in burned area over specific regions such as Northern Hemisphere Africa driven by human activity and agricultural expansion (Andela and van der Werf, 2014; Andela et al., 2017). Though we mainly focused on fire-climate interactions without consideration of human impacts in this study, the RESFire model is capable of reproducing the anthropogenic interference on fire activity as observed from the space (Zou et al., 2019). The carbon budget variables including GPP, NEP, and NEE increased by 4%, 7%, and 33%, respectively (Fig. 7c-d). These carbon variables affect terrestrial ecosystem productivity as well as fuel load supply for biomass burning, which further modulate fire emissions that lead to discrepancies between burned area and emission changes. For instance, most decreasing changes in burned area occurred in tropical and subtropical savannas and grasslands, while significant increasing changes were evident in boreal forest and tropical rainforests of Southeast Asia (Fig. 7a). This spatial shift of burning activity from low fuel loading areas (e.g., grassland) to high fuel loading areas (e.g., forest) greatly amplified the changes in fire emissions due to boosted fuel consumption. The complex climate-fire-ecosystem interactions will be discussed in the next section.

3.3 Simulations of climate-fire-ecosystem interactions using CESM-RESFire

In the last section, we found a 19% increase of global burned area in the RCP4.5 future scenario compared to the present-day scenario. We examined driving factors and spatial distributions of this increase in Fig. 8. The fire ignition distribution shows heterogeneous changes with significant increases in boreal forest regions over Eurasia as well as rainforest regions in South America but decreases in South American savanna, African rainforests, and savanna. These changes in fire ignition are mainly driven by changes in fuel combustibility as shown by fire combustion factors (Fig. 8b). The fire spread distribution (Fig. 8c) shows similar but more apparent patterns of increased fire spread rates over middle- to high-latitude regions but decreased fire spread rates over tropical regions, which is attributed to the changes in fire spread factors (Fig. 8d) modulated by surface temperature, precipitation, and relative humidity (Zou et al., 2019). The burned area changes are mainly driven by fire weather changes as suggested by fire spread rate variations because the increasing and decreasing areas in burned area (Fig. 7a) resemble the spatial pattern in fire spread rate changes (Fig. 8c). In other words, fire weather changes dominate burned area changes in the future and determine the changing tendencies of burning severity in these fire-prone regions. These burning activity changes found in this study also agree quite well with previous long-term projections based on an empirical statistical framework and a multi-model ensemble of 16 GCMs, in which they found good model agreement on increasing fire probabilities (~62%) at mid- to high-latitudes as well as decreasing fire probabilities (~20%) in the tropics (Moritz et al., 2012).

To understand changes in specific fire weather variables, we compared the differences of surface wind speed, surface temperature, rain precipitation and snow precipitation in Fig. 9. Most statistically significant wind speed changes occur over ocean areas rather than land areas (Fig. 9a), suggesting less impacts on fire spread and burned area changes. The regions with significantly increased burned areas (Fig. 7a) including boreal forests at high-latitude regions such as Siberia and Canada, rainforests in Southeast Asia, and savannas in Australia show suppressed precipitation in the future, especially rain precipitation (Fig. 9c). In contrast, the tropical regions with decreased burned areas in Fig. 7a also show increasing precipitation tendencies in the future scenario, suggesting strong associations of burning activity

Atmospheric Chemistry and Physics
Discussions

with precipitation changes. The relationship between burning activity and temperature changes is less intuitive in most regions except Australia (Fig. 9b), where shows both strong warming tendencies and largely increased burned areas. The complex relations between fire activity and fire weather variables will be discussed further.

The examination of fire, ecosystem, and fire weather variables suggested different feedback mechanisms in these interactions. To quantify different feedback pathways, we compared the sensitivity experiment results with the control runs and isolated atmosphere-centric and vegetation-centric feedback in Fig. 10. The comparison of the fire emission sensitivity experiments (CTRL2-SENS2A) revealed a positive feedback mechanism of fire activity (Fig. 10a) in that fire aerosols tend to suppress precipitation in most regions (Fig. 10b), which agrees well with satellite-based observations (Rosenfeld et al., 2019). It resulted in a 15.7 Mha yr^{-1} increase in global burned area simulations. On the contrary, the comparison of fire-induced land cover change experiments (SENS2A-SENS2B) suggested a negative feedback of fire activity (Fig. 10c) due to reduced fuel load supply (Fig. 10d) in post-fire vegetation changes with consideration of fire-induced LCC. After the incorporation of fire disturbance on land cover, global fuel loads decreased in many post-fire regions such as boreal forest in North America and tropical rainforests and led to a 10.2 Mha yr^{-1} decrease in global burned area (Table 5). The net feedback effect depends on a balance of these two opposite feedback mechanisms, which increases the complexity of climate-fire-ecosystem interactions at regional and global scales.

To further evaluate the detailed biophysical effects induced by fire-related LCC, we showed changes in fractional tree coverage, surface albedo, evapotranspiration, and total run-off between SENS2A and SENS2B in Fig. 11. Usually, large fires would induce a large amount of tree mortality in fire scorched regions, especially in the tropical and boreal forests, as shown in Fig. 11a. Since we simulated post-fire vegetation changes by converting dead tree covered regions to grasslands (if grasslands exist in the same grid cell) or bare land (if no grassland exists in the same grid cell) (Zou et al., 2019), these vegetation type and land cover change would trigger a series of ecological effects including changes in surface albedo (Fig. 11b), evapotranspiration (Fig. 11c), and run-off (Fig. 11d). These effects by deforestation might compensate biogeochemical warming effects of deforestation related carbon-cycle changes with a net cooling effect on a global scale (Bala et al., 2007;Jin et al., 2012;Randerson et al., 2006), but our simulation results here suggested almost neutral climate effects due to fire-induced LCC in both present-day and future scenarios (Table 2) that are less significant than previous findings.

Lastly, we examined climate impacts of biomass burning changes between the future and present-day scenarios in Fig. 12. Due to increased burning activity in many fire-prone regions in the RCP4.5 scenario, we found strongly enhanced AOD over high-latitude boreal forest regions, tropical forests in South America and Southeast Asia, and semi-arid regions in Australia (Fig. 12a). Increased fire aerosols led to different responses in cloud liquid water path, with large increases in high-latitude regions but generally decreases in the tropics and sub-tropics (Fig. 12b). They also resulted in pronounced changes in radiative effects due to aerosol-radiation (Fig. 12c) and aerosol-cloud interactions (Fig. 12d). Again, the changes in the latter are much stronger than the former. The fire-induced changes in RE_{ari} (Fig. 12c) show similar patterns with Fig. 3a, with generally cooling effects over the vicinities of fire areas and warming effects over the downwind regions. Similarly, the fire-induced changes in RE_{aci} (Fig. 12d) are consistent

https://doi.org/10.5194/acp-2019-646
Preprint. Discussion started: 4 September 2019

with Fig. 3b, with strong cooling effects at high-latitudes and warming effects in Southeast Asia and Australia due to local cloud changes (Fig. 12b).

4 Conclusions and implications

In this study, we conducted a series of fire-climate modeling experiments for the present and future projections with explicit simulations of multiple climate-fire-ecosystem feedback mechanisms. We evaluated the CESM-RESFire modeling performance in the context of fire-related radiative effects and terrestrial carbon balance. We summarized the fire radiative effects for the present-day and the RCP4.5 future scenarios in Fig. 13. We mainly considered fire-induced radiative effect changes related with fire aerosols and land cover change. We found that the fire radiative effect, which was caused by the increased global burning activity and subsequent aerosol-cloud interactions, increased from -0.59 ± 0.51 W m^{-2} in the 2000s to -1.60 ± 0.27 W m^{-2} in the 2050s. The global burned areas and fire carbon emissions increased by 19% and 100%, respectively, with large amplifications at boreal regions due to suppressed precipitation and enhanced fire spread rates. These changes imply increasing fire danger over high-latitude regions with prevalent peat lands, which will be more vulnerable to increased fire threats due to climate change. Potential increasing burning activity in these regions may greatly increase fire carbon and tracer gas and aerosol emissions that could have enormous impacts on terrestrial carbon balance and radiative budget. Our modeling results implied that the increase of fire aerosols could compensate the projected decrease of anthropogenic aerosols due to air pollution control policies in many regions (e.g., the eastern U.S. and China) (EPA, 2019;McClure and Jaffe, 2018;Wang et al., 2017;Zhao et al., 2014), where significant aerosol cooling effects dampened GHG warming effects (Goldstein et al., 2009;Rosenfeld et al., 2019). Such counteractive effect to anthropogenic emission reduction would also slow down air quality improvement and reduce associated health benefits revealed by previous studies (Markandya et al., 2018;Zhang et al., 2018).

Fire aerosol emissions and fire-induced land cover change manifest opposite feedback mechanisms in climate-fire-ecosystem interactions, showing a positive atmosphere-centric feedback induced by fire aerosol effects and a negative vegetation-centric feedback related with fire-induced land cover and fuel load change. These two distinct feedback mechanisms compete against each other and increase the complexity of interactions among each component. It is noted that we only included the atmosphere and land modeling components of the CESM model to investigate climate effects of global fires with other major components of the earth system including the ocean and sea/land ice in the prescribed data mode. Enhanced climate sensitivity and feedback and uncertainties on a multi-decadal scale might be expected in a fully coupled climate modeling system as previous studies revealed (Dunne et al., 2012;Dunne et al., 2013;Hazeleger et al., 2010;Andrews et al., 2012). We suggest more comprehensive evaluations at regional scales to investigate these complex interactions for major fire-prone regions. We also need to advance fire modeling capability by integrating more fire-related processes and climate effects such as fire emitted brown carbon (Brown et al., 2018;Feng et al., 2013;Forrister et al., 2015;Liu et al., 2015;Wang et al., 2018;Zhang et al., 2017; Zhang et al., 2019) and fire-vegetation-climate interactions and teleconnections (Garcia et al., 2016;Stark et al., 2016). More evaluation metrics such as large wildfire extreme events should be considered in future studies to improve our understanding of fire activity, their variations and trends, and their relationship with decadal climate change.

Atmospheric Chemistry and Physics Discussions
Open Access
EGU

Code and data availability

The Level-3 MODIS monthly AOD data from the Aqua platform (MYD08_M3, http://dx.doi.org/10.5067/MODIS/MYD08_M3.006) used for model evaluation are available via NASA Level-1 and Atmosphere Archive & Distribution System (LAADS) Distributed Active Archive Center (DAAC) in https://ladsweb.modaps.eosdis.nasa.gov/missions-and-measurements/products/MYD08_M3/. The AERONET Version 3 Level 2.0 AOT data are available at https://aeronet.gsfc.nasa.gov/. The GFED burned area and fire emission datasets are available at http://www.globalfiredata.org/. All the CESM-RESFire model input and output data reported in the paper are tabulated in the main text and archived on the Cheyenne high-performance computing system (doi:10.5065/D6RX99HX) and High-Performance Storage System (HPSS) managed by the Computational & Information Systems Lab (CISL) of NCAR. The modeling source code and data materials are available upon request, which should be addressed to Y. Wang (yuhang.wang@eas.gatech.edu).

Author contribution

Y. Zou and Y. Wang designed the experiments and Y. Zou carried them out. Y. Zou developed the model code and performed the simulations. Y. Zou prepared the manuscript and all co-authors reviewed and edited the manuscript.

Competing interests

The authors declare that they have no conflict of interest.

Acknowledgments

This work was supported by the National Science Foundation (NSF) through grant 1243220 and by the U.S. Department of Energy (DOE)'s office of Science as part of the Regional and Global Climate Modeling Program (NSF-DOE-USDA EaSM2). The Pacific Northwest National Laboratory (PNNL) is operated for DOE by Battelle Memorial Institute under contract DE-AC05-76RL01830. H. Tian was supported by the NSF through grant 1243232. It has not been subjected to any NSF review and therefore does not necessarily reflect the views of the Foundation, and no official endorsement should be inferred.
We would like to acknowledge high-performance computing support from Cheyenne (doi:10.5065/D6RX99HX) provided by NCAR's CISL, sponsored by the National Science Foundation. We are thankful to Steve Platnick for processing the MODIS AOD data. We thank all the GFED team members for providing the GFED data at http://www.globalfiredata.org/. We thank Wei Min Hao, Brent Holben, Paulo Artaxo, Mikhail Panchenko, Sergey Sakerin, Rachel T. Pinker and their staff for establishing and maintaining the six AERONET sites used in this study. We thank Chandan Sarangi for the helpful discussion to improve the presentation of this work.

References

Abatzoglou, J. T., and Williams, A. P.: Impact of anthropogenic climate change on wildfire across western US forests, P. Natl. Acad. Sci. USA, 113, 11770-11775, 10.1073/pnas.1607171113, 2016.

Abatzoglou, J. T., Williams, A. P., and Barbero, R.: Global Emergence of Anthropogenic Climate Change in Fire Weather Indices, Geophys. Res. Lett., 46, 326-336, 10.1029/2018gl080959, 2019.

Abel, S. J., Highwood, E. J., Haywood, J. M., and Stringer, M. A.: The direct radiative effect of biomass burning aerosols over southern Africa, Atmos. Chem. Phys., 5, 1999-2018, DOI 10.5194/acp-5-1999-2005, 2005.

Andela, N., Morton, D. C., Giglio, L., Chen, Y., van der Werf, G. R., Kasibhatla, P. S., DeFries, R. S., Collatz, G. J., Hantson, S., Kloster, S., Bachelet, D., Forrest, M., Lasslop, G., Li, F., Mangeon, S., Melton, J. R., Yue, C., Randerson, J. T.: A human-driven decline in global burned area, Science, 356(6345), 1356–1362. https://doi.org/10.1126/science.aal4108, 2017.

Andela, N., and van der Werf, G. R.: Recent trends in African fires driven by cropland expansion and El Nino to La Nina transition, Nature Climate Change, 4, 791–795. https://doi.org/10.1038/nclimate2313, 2014.

Andrews, T., Gregory, J. M., Webb, M. J., and Taylor, K. E.: Forcing, feedbacks and climate sensitivity in CMIP5 coupled atmosphere-ocean climate models, Geophys. Res. Lett., 39, Artn L0971210.1029/2012gl051607, 2012.

Bala, G., Caldeira, K., Wickett, M., Phillips, T. J., Lobell, D. B., Delire, C., and Mirin, A.: Combined climate and carbon-cycle effects of large-scale deforestation, P. Natl. Acad. Sci. USA, 104, 6550-6555, 10.1073/pnas.0608998104, 2007.

Barbero, R., Abatzoglou, J. T., Larkin, N. K., Kolden, C. A., and Stocks, B.: Climate change presents increased potential for very large fires in the contiguous United States, Int. J. Wildland Fire, 24, 892-899, 10.1071/Wf15083, 2015.

Bowman, D. M. J. S., Balch, J. K., Artaxo, P., Bond, W. J., Carlson, J. M., Cochrane, M. A., D'Antonio, C. M., DeFries, R. S., Doyle, J. C., Harrison, S. P., Johnston, F. H., Keeley, J. E., Krawchuk, M. A., Kull, C. A., Marston, J. B., Moritz, M. A., Prentice, I. C., Roos, C. I., Scott, A. C., Swetnam, T. W., van der Werf, G. R., and Pyne, S. J.: Fire in the Earth System, Science, 324, 481-484, 10.1126/science.1163886, 2009.

Brown, H., Liu, X. H., Feng, Y., Jiang, Y. Q., Wu, M. X., Lu, Z., Wu, C. L., Murphy, S., and Pokhrel, R.: Radiative effect and climate impacts of brown carbon with the Community Atmosphere Model (CAM5), Atmos. Chem. Phys., 18, 17745-17768, 10.5194/acp-18-17745-2018, 2018.

Ciais, P., C. Sabine, G. Bala, L. Bopp, V. Brovkin, J. Canadell, A. Chhabra, R. DeFries, J. Galloway, M. Heimann, C. Jones, C. Le Quéré, R.B. Myneni, and Thornton, S. P. a. P.: Carbon and Other Biogeochemical Cycles in Climate Change 2013: The Physical Science Basis, Cambridge, United Kingdom and New York, NY, USA, 2013.

Clarke, H., Lucas, C., and Smith, P.: Changes in Australian fire weather between 1973 and 2010, Int. J. Climatol., 33, 931-944, 10.1002/joc.3480, 2013.

Computational and Information Systems Laboratory (CISL). Cheyenne: HPE/SGI ICE XA System (University Community Computing). Boulder, CO: National Center for Atmospheric Research. doi:10.5065/D6RX99HX, 2017.

https://doi.org/10.5194/acp-2019-646
Preprint. Discussion started: 4 September 2019

Atmospheric Chemistry and Physics Discussions

Dennison, P. E., Brewer, S. C., Arnold, J. D., and Moritz, M. A.: Large wildfire trends in the western United States, 1984-2011, Geophys. Res. Lett., 41, 2928-2933, 10.1002/2014gl059576, 2014.

Dentener, F., Kinne, S., Bond, T., Boucher, O., Cofala, J., Generoso, S., Ginoux, P., Gong, S., Hoelzemann, J. J., Ito, A., Marelli, L., Penner, J. E., Putaud, J. P., Textor, C., Schulz, M., van der Werf, G. R., and Wilson, J.: Emissions of primary aerosol and precursor gases in the years 2000 and 1750 prescribed data-sets for AeroCom, Atmos. Chem. Phys., 6, 4321-4344, DOI 10.5194/acp-6-4321-2006, 2006.

Dunne, J. P., John, J. G., Adcroft, A. J., Griffies, S. M., Hallberg, R. W., Shevliakova, E., Stouffer, R. J., Cooke, W., Dunne, K. A., Harrison, M. J., Krasting, J. P., Malyshev, S. L., Milly, P. C. D., Phillipps, P. J., Sentman, L. T., Samuels, B. L., Spelman, M. J., Winton, M., Wittenberg, A. T., and Zadeh, N.: GFDL's ESM2 Global Coupled Climate-Carbon Earth System Models. Part I: Physical Formulation and Baseline Simulation Characteristics, J. Climate, 25, 6646-6665, 10.1175/Jcli-D-11-00560.1, 2012.

Dunne, J. P., John, J. G., Shevliakova, E., Stouffer, R. J., Krasting, J. P., Malyshev, S. L., Milly, P. C. D., Sentman, L. T., Adcroft, A. J., Cooke, W., Dunne, K. A., Griffies, S. M., Hallberg, R. W., Harrison, M. J., Levy, H., Wittenberg, A. T., Phillips, P. J., and Zadeh, N.: GFDL's ESM2 Global Coupled Climate-Carbon Earth System Models. Part II: Carbon System Formulation and Baseline Simulation Characteristics, J. Climate, 26, 2247-2267, 10.1175/Jcli-D-12-00150.1, 2013.

Particulate Matter (PM2.5) trends: https://www.epa.gov/air-trends/particulate-matter-pm25-trends, access: Feburary 19, 2019.

Fann, N., Alman, B., Broome, R. A., Morgan, G. G., Johnston, F. H., Pouliot, G., and Rappold, A. G.: The health impacts and economic value of wildland fire episodes in the US: 2008-2012, Sci. Total. Environ., 610, 802-809, 10.1016/j.scitotenv.2017.08.024, 2018.

Feng, Y., Ramanathan, V., and Kotamarthi, V. R.: Brown carbon: a significant atmospheric absorber of solar radiation?, Atmos. Chem. Phys., 13, 8607-8621, 10.5194/acp-13-8607-2013, 2013.

Flanner, M. G., and Zender, C. S.: Snowpack radiative heating: Influence on Tibetan Plateau climate, Geophys. Res. Lett., 32, Artn L0650110.1029/2004gl022076, 2005.

Flannigan, M., Cantin, A. S., de Groot, W. J., Wotton, M., Newbery, A., and Gowman, L. M.: Global wildland fire season severity in the 21st century, Forest Ecol. Manag., 294, 54-61, 10.1016/j.foreco.2012.10.022, 2013.

Flannigan, M. D., Krawchuk, M. A., de Groot, W. J., Wotton, B. M., and Gowman, L. M.: Implications of changing climate for global wildland fire, Int. J. Wildland Fire, 18, 483-507, 10.1071/Wf08187, 2009.

Forrister, H., Liu, J., Scheuer, E., Dibb, J., Ziemba, L., Thornhill, K. L., Anderson, B., Diskin, G., Perring, A. E., Schwarz, J. P., Campuzano-Jost, P., Day, D. A., Palm, B. B., Jimenez, J. L., Nenes, A., and Weber, R. J.: Evolution of brown carbon in wildfire plumes, Geophys. Res. Lett., 42, 4623-4630, 10.1002/2015gl063897, 2015.

Garcia, E. S., Swann, A. L. S., Villegas, J. C., Breshears, D. D., Law, D. J., Saleska, S. R., and Stark, S. C.: Synergistic Ecoclimate Teleconnections from Forest Loss in Different Regions Structure Global Ecological Responses, Plos One, 11, ARTN e016504210.1371/journal.pone.0165042, 2016.

Ghan, S. J.: Technical Note: Estimating aerosol effects on cloud radiative forcing, Atmos. Chem. Phys., 13, 9971-9974, 10.5194/acp-13-9971-2013, 2013.

Giglio, L., Randerson, J. T., and van der Werf, G. R.: Analysis of daily, monthly, and annual burned area using the fourth-generation global fire emissions database (GFED4), J. Geophys. Res.-Biogeo., 118, 317-328, 10.1002/jgrg.20042, 2013.

Gilardoni, S., Vignati, E., Marmer, E., Cavalli, F., Belis, C., Gianelle, V., Loureiro, A., and Artaxo, P.: Sources of carbonaceous aerosol in the Amazon basin, Atmos. Chem. Phys., 11, 2747-2764, 10.5194/acp-11-2747-2011, 2011.

Goldstein, A. H., Koven, C. D., Heald, C. L., and Fung, I. Y.: Biogenic carbon and anthropogenic pollutants combine to form a cooling haze over the southeastern United States, P. Natl. Acad. Sci. USA, 106, 8835-8840, 10.1073/pnas.0904128106, 2009.

Hall, J. R.: The total cost of fire in the United States, National Fire Protection Association, Quincy, MA, 38, 2014.

Hantson, S., Arneth, A., Harrison, S. P., Kelley, D. I., Prentice, I. C., Rabin, S. S., Archibald, S., Mouillot, F., Arnold, S. R., Artaxo, P., Bachelet, D., Ciais, P., Forrest, M., Friedlingstein, P., Hickler, T., Kaplan, J. O., Kloster, S., Knorr, W., Lasslop, G., Li, F., Mangeon, S., Melton, J. R., Meyn, A., Sitch, S., Spessa, A., van der Werf, G. R., Voulgarakis, A., and Yue, C.: The status and challenge of global fire modelling, Biogeosciences, 13, 3359-3375, 10.5194/bg-13-3359-2016, 2016.

Harris, R. M. B., Remenyi, T. A., Williamson, G. J., Bindoff, N. L., and Bowman, D. M. J. S.: Climate-vegetation-fire interactions and feedbacks: trivial detail or major barrier to projecting the future of the Earth system?, Wires Clim. Change, 7, 910-931, 10.1002/wcc.428, 2016.

Hazeleger, W., Severijns, C., Semmler, T., Stefanescu, S., Yang, S. T., Wang, X. L., Wyser, K., Dutra, E., Baldasano, J. M., Bintanja, R., Bougeault, P., Caballero, R., Ekman, A. M. L., Christensen, J. H., van den Hurk, B., Jimenez, P., Jones, C., Kallberg, P., Koenigk, T., McGrath, R., Miranda, P., Van Noije, T., Palmer, T., Parodi, J. A., Schmith, T., Selten, F., Storelvmo, T., Sterl, A., Tapamo, H., Vancoppenolle, M., Viterbo, P., and Willen, U.: EC-Earth A Seamless Earth-System Prediction Approach in Action, B. Am. Meteorol. Soc., 91, 1357-1363, 10.1175/2010bams2877.1, 2010.

Hurrell, J. W., Holland, M. M., Gent, P. R., Ghan, S., Kay, J. E., Kushner, P. J., Lamarque, J. F., Large, W. G., Lawrence, D., Lindsay, K., Lipscomb, W. H., Long, M. C., Mahowald, N., Marsh, D. R., Neale, R. B., Rasch, P., Vavrus, S., Vertenstein, M., Bader, D., Collins, W. D., Hack, J. J., Kiehl, J., and Marshall, S.: The Community Earth System Model A Framework for Collaborative Research, B. Am. Meteorol. Soc., 94, 1339-1360, 10.1175/Bams-D-12-00121.1, 2013.

Hurteau, M. D., Westerling, A. L., Wiedinmyer, C., and Bryant, B. P.: Projected Effects of Climate and Development on California Wildfire Emissions through 2100, Environ. Sci. Technol., 48, 2298-2304, 10.1021/es4050133, 2014.

Hurtt, G. C., Frolking, S., Fearon, M. G., Moore, B., Shevliakova, E., Malyshev, S., Pacala, S. W., and Houghton, R. A.: The underpinnings of land-use history: three centuries of global gridded land-use transitions, wood-harvest activity, and resulting secondary lands, Global Change Biol., 12, 1208-1229, 10.1111/j.1365-2486.2006.01150.x, 2006.

https://doi.org/10.5194/acp-2019-646
Preprint. Discussion started: 4 September 2019

Jiang, Y. Q., Lu, Z., Liu, X. H., Qian, Y., Zhang, K., Wang, Y. H., and Yang, X. Q.: Impacts of global open-fire aerosols on direct radiative, cloud and surface-albedo effects simulated with CAM5, Atmos. Chem. Phys., 16, 14805-14824, 10.5194/acp-16-14805-2016, 2016.

Jin, Y. F., Randerson, J. T., Goetz, S. J., Beck, P. S. A., Loranty, M. M., and Goulden, M. L.: The influence of burn severity on postfire vegetation recovery and albedo change during early succession in North American boreal forests, J. Geophys. Res.-Biogeo., 117, Artn G0103610.1029/2011jg001886, 2012.

Johnston, F. H., Henderson, S. B., Chen, Y., Randerson, J. T., Marlier, M., DeFries, R. S., Kinney, P., Bowman, D. M. J. S., and Brauer, M.: Estimated Global Mortality Attributable to Smoke from Landscape Fires, Environ. Health Persp., 120, 695-701, 10.1289/ehp.1104422, 2012.

Jolly, W. M., Cochrane, M. A., Freeborn, P. H., Holden, Z. A., Brown, T. J., Williamson, G. J., and Bowman, D. M. J. S.: Climate-induced variations in global wildfire danger from 1979 to 2013, Nat. Commun., 6, ARTN 753710.1038/ncomms8537, 2015.

Ke, Z., Wang, Y., Zou, Y., Song, Y., and Liu, Y.: The global plume-rise dataset and its climate model implement, submitted to J. Adv. Model Earth Sy., 2019.

Kloster, S., Mahowald, N. M., Randerson, J. T., Thornton, P. E., Hoffman, F. M., Levis, S., Lawrence, P. J., Feddema, J. J., Oleson, K. W., and Lawrence, D. M.: Fire dynamics during the 20th century simulated by the Community Land Model, Biogeosciences, 7, 1877-1902, 10.5194/bg-7-1877-2010, 2010.

Kloster, S., Mahowald, N. M., Randerson, J. T., and Lawrence, P. J.: The impacts of climate, land use, and demography on fires during the 21st century simulated by CLM-CN, Biogeosciences, 9, 509-525, 10.5194/bg-9-509-2012, 2012.

Kurokawa, J., Ohara, T., Morikawa, T., Hanayama, S., Janssens-Maenhout, G., Fukui, T., Kawashima, K., and Akimoto, H.: Emissions of air pollutants and greenhouse gases over Asian regions during 2000-2008: Regional Emission inventory in ASia (REAS) version 2, Atmos. Chem. Phys., 13, 11019-11058, 10.5194/acp-13-11019-2013, 2013.

Lamarque, J. F., Bond, T. C., Eyring, V., Granier, C., Heil, A., Klimont, Z., Lee, D., Liousse, C., Mieville, A., Owen, B., Schultz, M. G., Shindell, D., Smith, S. J., Stehfest, E., Van Aardenne, J., Cooper, O. R., Kainuma, M., Mahowald, N., McConnell, J. R., Naik, V., Riahi, K., and van Vuuren, D. P.: Historical (1850-2000) gridded anthropogenic and biomass burning emissions of reactive gases and aerosols: methodology and application, Atmos. Chem. Phys., 10, 7017-7039, 10.5194/acp-10-7017-2010, 2010.

Le Quere, C., Andres, R. J., Boden, T., Conway, T., Houghton, R. A., House, J. I., Marland, G., Peters, G. P., van der Werf, G. R., Ahlstrom, A., Andrew, R. M., Bopp, L., Canadell, J. G., Ciais, P., Doney, S. C., Enright, C., Friedlingstein, P., Huntingford, C., Jain, A. K., Jourdain, C., Kato, E., Keeling, R. F., Goldewijk, K. K., Levis, S., Levy, P., Lomas, M., Poulter, B., Raupach, M. R., Schwinger, J., Sitch, S., Stocker, B. D., Viovy, N., Zaehle, S., and Zeng, N.: The global carbon budget 1959-2011, Earth Syst. Sci. Data, 5, 165-185, 10.5194/essd-5-165-2013, 2013.

https://doi.org/10.5194/acp-2019-646
Preprint. Discussion started: 4 September 2019

Atmospheric Chemistry and Physics Discussions

Li, F., Levis, S., and Ward, D. S.: Quantifying the role of fire in the Earth system - Part 1: Improved global fire modeling in the Community Earth System Model (CESM1), Biogeosciences, 10, 2293-2314, 10.5194/bg-10-2293-2013, 2013.

Li, F., Bond-Lamberty, B., and Levis, S.: Quantifying the role of fire in the Earth system - Part 2: Impact on the net carbon balance of global terrestrial ecosystems for the 20th century, Biogeosciences, 11, 1345-1360, 10.5194/bg-11-1345-2014, 2014.

Liu, J., Scheuer, E., Dibb, J., Diskin, G. S., Ziemba, L. D., Thornhill, K. L., Anderson, B. E., Wisthaler, A., Mikoviny, T., Devi, J. J., Bergin, M., Perring, A. E., Markovic, M. Z., Schwarz, J. P., Campuzano-Jost, P., Day, D. A., Jimenez, J. L., and Weber, R. J.: Brown carbon aerosol in the North American continental troposphere: sources, abundance, and radiative forcing, Atmos. Chem. Phys., 15, 7841-7858, 10.5194/acp-15-7841-2015, 2015.

Liu, X., Easter, R. C., Ghan, S. J., Zaveri, R., Rasch, P., Shi, X., Lamarque, J. F., Gettelman, A., Morrison, H., Vitt, F., Conley, A., Park, S., Neale, R., Hannay, C., Ekman, A. M. L., Hess, P., Mahowald, N., Collins, W., Iacono, M. J., Bretherton, C. S., Flanner, M. G., and Mitchell, D.: Toward a minimal representation of aerosols in climate models: description and evaluation in the Community Atmosphere Model CAM5, Geosci. Model Dev., 5, 709-739, 10.5194/gmd-5-709-2012, 2012.

Liu, Y., Zhang, K., Qian, Y., Wang, Y., Zou, Y., Song, Y., Wan, H., Liu, X., and Yang, X.-Q.: Investigation of short-term effective radiative forcing of fire aerosols over North America using nudged hindcast ensembles, Atmos. Chem. Phys., 18, 31-47, 10.5194/acp-18-31-2018, 2018.

Liu, Y. Q.: New development and application needs for Earth system modeling of fire-climate-ecosystem interactions, Environ. Res. Lett., 13, ARTN 01100110.1088/1748-9326/aaa347, 2018.

Liu, Y. Q., Stanturf, J., and Goodrick, S.: Trends in global wildfire potential in a changing climate, Forest Ecol. Manag., 259, 685-697, 10.1016/j.foreco.2009.09.002, 2010.

Markandya, A., Sampedro, J., Smith, S. J., Dingenen, R. V., Pizarro-Irizar, C., Arto, I., and González-Eguino, M.: Health co-benefits from air pollution and mitigation costs of the Paris Agreement: a modelling study, The Lancet Planetary Health, 2, e126-e133, https://doi.org/10.1016/S2542-5196(18)30029-9, 2018.

Martin, M. V., Logan, J. A., Kahn, R. A., Leung, F. Y., Nelson, D. L., and Diner, D. J.: Smoke injection heights from fires in North America: analysis of 5 years of satellite observations, Atmos. Chem. Phys., 10, 1491-1510, 2010.

McClure, C. D., and Jaffe, D. A.: US particulate matter air quality improves except in wildfire-prone areas, P. Natl. Acad. Sci. USA, 115, 7901-7906, 10.1073/pnas.1804353115, 2018.

Moritz, M. A., Parisien, M. A., Batllori, E., Krawchuk, M. A., Van Dorn, J., Ganz, D. J., and Hayhoe, K.: Climate change and disruptions to global fire activity, Ecosphere, 3, Unsp 4910.1890/Es11-00345.1, 2012.

Neale, R. B., Chen, C. C., Gettelman, A., Lauritzen, P. H., Park, S., Williamson, D. L., Conley, A. J., Garcia, R., Kinnison, D., Lamarque, J. F., Marsh, D., Mills, M., Smith, A. K., Tilmes, S., Vitt, F., Morrison, H., Cameron-Smith, P., Collins, W. D., Iacono, M. J., Easter, R. C., Ghan, S. J., Liu, X. H., Rasch, P. J., and Taylor, M. A.: Description of the NCAR Community Atmosphere Model (CAM 5.0), NCAR 289, 2013.

Oleson, K. W., Lawrence, D. M., Bonan, G. B., Drewniak, B., Huang, M., Koven, C. D., Levis, S., Li, F., Riley, W. J., Subin, Z. M., Swenson, S. C., Thornton, P. E., Bozbiyik, A., Fisher, R., Heald, C. L., Kluzek, E., Lamarque, J.-

F., Lawrence, P. J., Leung, L. R., Lipscomb, W., Muszala, S., Ricciuto, D. M., Sacks, W., Sun, Y., Tang, J., and Yang, Z.-L.: Technical description of version 4.5 of the Community Land Model (CLM), NCAR 434, 2013.

Park, S., Bretherton, C. S., and Rasch, P. J.: Integrating Cloud Processes in the Community Atmosphere Model, Version 5, J. Climate, 27, 6821-6856, 10.1175/Jcli-D-14-00087.1, 2014.

Parks, S. A., Miller, C., Abatzoglou, J. T., Holsinger, L. M., Parisien, M. A., and Dobrowski, S. Z.: How will climate change affect wildland fire severity in the western US?, Environ. Res. Lett., 11, Artn 03500210.1088/1748-9326/11/3/035002, 2016.

Pellegrini, A. F. A., Ahlstrom, A., Hobbie, S. E., Reich, P. B., Nieradzik, L. P., Staver, A. C., Scharenbroch, B. C., Jumpponen, A., Anderegg, W. R. L., Randerson, J. T., and Jackson, R. B.: Fire frequency drives decadal changes in soil carbon and nitrogen and ecosystem productivity, Nature, 553, 194-198, 10.1038/nature24668, 2018.

Piao, S. L., Sitch, S., Ciais, P., Friedlingstein, P., Peylin, P., Wang, X. H., Ahlstrom, A., Anav, A., Canadell, J. G., Cong, N., Huntingford, C., Jung, M., Levis, S., Levy, P. E., Li, J. S., Lin, X., Lomas, M. R., Lu, M., Luo, Y. Q., Ma, Y. C., Myneni, R. B., Poulter, B., Sun, Z. Z., Wang, T., Viovy, N., Zaehle, S., and Zeng, N.: Evaluation of terrestrial carbon cycle models for their response to climate variability and to CO2 trends, Global Change Biol., 19, 2117-2132, 10.1111/gcb.12187, 2013.

Quillet, A., Peng, C, Garneau, M.: Toward dynamic global vegetation models for simulating vegetation–climate interactions and feedbacks: recent developments, limitations, and future challenges, Environmental Reviews, 18(NA), 333-53, 10.1139/A10-016, 2010.

Randerson, J. T., Liu, H., Flanner, M. G., Chambers, S. D., Jin, Y., Hess, P. G., Pfister, G., Mack, M. C., Treseder, K. K., Welp, L. R., Chapin, F. S., Harden, J. W., Goulden, M. L., Lyons, E., Neff, J. C., Schuur, E. A. G., and Zender, C. S.: The impact of boreal forest fire on climate warming, Science, 314, 1130-1132, 10.1126/science.1132075, 2006.

Randerson, J. T., Chen, Y., van der Werf, G. R., Rogers, B. M., and Morton, D. C.: Global burned area and biomass burning emissions from small fires, J. Geophys. Res.-Biogeo., 117, Artn G0401210.1029/2012jg002128, 2012.

Rayner, N. A., Parker, D. E., Horton, E. B., Folland, C. K., Alexander, L. V., Rowell, D. P., Kent, E. C., and Kaplan, A.: Global analyses of sea surface temperature, sea ice, and night marine air temperature since the late nineteenth century, J. Geophys. Res.-Atmos., 108, Artn 440710.1029/2002jd002670, 2003.

Platnick, S., Hubanks, P., Meyer, K., and King, M. D.: MODIS Atmosphere L3 Monthly Product. NASA MODIS Adaptive Processing System, Goddard Space Flight Center, USA: http://dx.doi.org/10.5067/MODIS/MYD08_M3.061, 2015.

Richardson, L. A., Champ, P. A., and Loomis, J. B.: The hidden cost of wildfires: Economic valuation of health effects of wildfire smoke exposure in Southern California, J. Forest. Econ., 18, 14-35, 10.1016/j.jfe.2011.05.002, 2012.

Ridley, D. A., Heald, C. L., Kok, J. F., and Zhao, C.: An observationally constrained estimate of global dust aerosol optical depth, Atmos. Chem. Phys., 16, 15097-15117, 10.5194/acp-16-15097-2016, 2016.

Rosenfeld, D., Zhu, Y. N., Wang, M. H., Zheng, Y. T., Goren, T., and Yu, S. C.: Aerosol-driven droplet concentrations dominate coverage and water of oceanic low-level clouds, Science, 363, 599-+, ARTN eaav056610.1126/science.aav0566, 2019.

Seidl, R., Thom, D., Kautz, M., Martin-Benito, D., Peltoniemi, M., Vacchiano, G., Wild, J., Ascoli, D., Petr, M., Honkaniemi, J., Lexer, M. J., Trotsiuk, V., Mairota, P., Svoboda, M., Fabrika, M., Nagel, T. A., and Reyer, C. P. O.: Forest disturbances under climate change, Nat. Clim. Change, 7, 395-402, 10.1038/Nclimate3303, 2017.

Seo, H., and Kim, Y.: Interactive impacts of fire and vegetation dynamics on global carbon and water budget using Community Land Model version 4.5, Geosci. Model. Dev., 12, 457-472, 10.5194/gmd-12-457-2019, 2019.

Shuman, J. K., Foster, A. C., Shugart, H. H., Hoffman-Hall, A., Krylov, A., Loboda, T., Ershov, D., and Sochilova, E.: Fire disturbance and climate change: implications for Russian forests, Environ. Res. Lett., 12, ARTN 03500310.1088/1748-9326/aa5eed, 2017.

Sofiev, M., Ermakova, T., and Vankevich, R.: Evaluation of the smoke-injection height from wild-land fires using remote-sensing data, Atmos. Chem. Phys., 12, 1995-2006, 10.5194/acp-12-1995-2012, 2012.

Stark, S. C., Breshears, D. D., Garcia, E. S., Law, D. J., Minor, D. M., Saleska, S. R., Swann, A. L. S., Villegas, J. C., Aragao, L. E. O. C., Bella, E. M., Borma, L. S., Cobb, N. S., Litvak, M. E., Magnusson, W. E., Morton, J. M., and Redmond, M. D.: Toward accounting for ecoclimate teleconnections: intra- and inter-continental consequences of altered energy balance after vegetation change, Landscape Ecol., 31, 181-194, 10.1007/s10980-015-0282-5, 2016.

Sun, Y., Gu, L. H., and Dickinson, R. E.: A numerical issue in calculating the coupled carbon and water fluxes in a climate model, J. Geophys. Res.-Atmos., 117, Artn D2210310.1029/2012jd018059, 2012.

Thomas, D., Butry, D., Gilbert, S., Webb, D., and Fung, J.: The costs and losses of wildfires: A literature review, National Institute of Standards and Technology, 72, 2017.

Thonicke, K., Spessa, A., Prentice, I. C., Harrison, S. P., Dong, L., and Carmona-Moreno, C.: The influence of vegetation, fire spread and fire behaviour on biomass burning and trace gas emissions: results from a process-based model, Biogeosciences, 7, 1991-2011, 10.5194/bg-7-1991-2010, 2010.

Tosca, M. G., Randerson, J. T., and Zender, C. S.: Global impact of smoke aerosols from landscape fires on climate and the Hadley circulation, Atmos. Chem. Phys., 13, 5227-5241, 10.5194/acp-13-5227-2013, 2013.

van der Werf, G. R., Randerson, J. T., Giglio, L., Collatz, G. J., Kasibhatla, P. S., and Arellano, A. F.: Interannual variability in global biomass burning emissions from 1997 to 2004, Atmos. Chem. Phys., 6, 3423-3441, DOI 10.5194/acp-6-3423-2006, 2006.

van der Werf, G. R., Randerson, J. T., Giglio, L., van Leeuwen, T. T., Chen, Y., Rogers, B. M., Mu, M. Q., van Marle, M. J. E., Morton, D. C., Collatz, G. J., Yokelson, R. J., and Kasibhatla, P. S.: Global fire emissions estimates during 1997-2016, Earth Syst. Sci. Data, 9, 697-720, 10.5194/essd-9-697-2017, 2017.

Wang, J. D., Zhao, B., Wang, S. X., Yang, F. M., Xing, J., Morawska, L., Ding, A. J., Kulmala, M., Kerminen, V. M., Kujansuu, J., Wang, Z. F., Ding, D. A., Zhang, X. Y., Wang, H. B., Tian, M., Petaja, T., Jiang, J. K., and Hao, J. M.: Particulate matter pollution over China and the effects of control policies, Sci. Total Environ., 584, 426-447, 10.1016/j.scitotenv.2017.01.027, 2017.

Wang, X., Heald, C. L., Liu, J. M., Weber, R. J., Campuzano-Jost, P., Jimenez, J. L., Schwarz, J. P., and Perring, A. E.: Exploring the observational constraints on the simulation of brown carbon, Atmos. Chem. Phys., 18, 635-653, 10.5194/acp-18-635-2018, 2018.

https://doi.org/10.5194/acp-2019-646
Preprint. Discussion started: 4 September 2019

Ward, D. S., Kloster, S., Mahowald, N. M., Rogers, B. M., Randerson, J. T., and Hess, P. G.: The changing radiative forcing of fires: global model estimates for past, present and future, Atmos. Chem. Phys., 12, 10857-10886, 10.5194/acp-12-10857-2012, 2012.

Westerling, A. L., Hidalgo, H. G., Cayan, D. R., and Swetnam, T. W.: Warming and earlier spring increase western US forest wildfire activity, Science, 313, 940-943, 10.1126/science.1128834, 2006.

Wotton, B. M., Flannigan, M. D., and Marshall, G. A.: Potential climate change impacts on fire intensity and key wildfire suppression thresholds in Canada, Environ. Res. Lett., 12, ARTN 09500310.1088/1748-9326/aa7e6e, 2017.

Yang, G., Di, X. Y., Guo, Q. X., Shu, Z., Zeng, T., Yu, H. Z., and Wang, C.: The impact of climate change on forest fire danger rating in China's boreal forest, J. For. Res., 22, 249-257, 10.1007/s11676-011-0158-8, 2011.

Yang, J., Tian, H. Q., Tao, B., Ren, W., Pan, S. F., Liu, Y. Q., and Wang, Y. H.: A growing importance of large fires in conterminous United States during 1984-2012, J. Geophys. Res.-Biogeo., 120, 2625-2640, 10.1002/2015jg002965, 2015.

Young, A. M., Higuera, P. E., Duffy, P. A., and Hu, F. S.: Climatic thresholds shape northern high-latitude fire regimes and imply vulnerability to future climate change, Ecography., 40, 606-617, 10.1111/ecog.02205, 2017.

Yue, C., Ciais, P., Cadule, P., Thonicke, K., and van Leeuwen, T. T.: Modelling the role of fires in the terrestrial carbon balance by incorporating SPITFIRE into the global vegetation model ORCHIDEE - Part 2: Carbon emissions and the role of fires in the global carbon balance, Geosci. Model Dev., 8, 1321-1338, 10.5194/gmd-8-1321-2015, 2015.

Yue, C., Ciais, P., Zhu, D., Wang, T., Peng, S. S., and Piao, S. L.: How have past fire disturbances contributed to the current carbon balance of boreal ecosystems?, Biogeosciences, 13, 675-690, 10.5194/bg-13-675-2016, 2016.

Yue, X., Mickley, L. J., Logan, J. A., and Kaplan, J. O.: Ensemble projections of wildfire activity and carbonaceous aerosol concentrations over the western United States in the mid-21st century, Atmos. Environ., 77, 767-780, 10.1016/j.atmosenv.2013.06.003, 2013.

Zhang, A., Wang, Y., Zhang, Y., Weber, R. J., Song, Y., Ke, Z., and Zou, Y.: Modeling global radiative effect of brown carbon: A larger heating source in the tropical free troposphere than black carbon, Atmos. Chem. Phys. Discuss., https://doi.org/10.5194/acp-2019-594, in review, 2019.

Zhang, Y., West, J. J., Mathur, R., Xing, J., Hogrefe, C., Roselle, S. J., Bash, J. O., Pleim, J. E., Gan, C.-M., and Wong, D. C.: Long-term trends in the ambient $PM_{2.5}$- and O_3-related mortality burdens in the United States under emission reductions from 1990 to 2010, Atmos. Chem. Phys., 18, 15003-15016, https://doi.org/10.5194/acp-18-15003-2018, 2018.

Zhang, Y. Z., Forrister, H., Liu, J. M., Dibb, J., Anderson, B., Schwarz, J. P., Perring, A. E., Jimenez, J. L., Campuzano-Jost, P., Wang, Y. H., Nenes, A., and Weber, R. J.: Top-of-atmosphere radiative forcing affected by brown carbon in the upper troposphere, Nat. Geosci., 10, 486-+, 10.1038/Ngeo2960, 2017.

Zhang, Z., Meyer, K., Yu, H., Platnick, S., Colarco, P., Liu, Z., and Oreopoulos, L.: Shortwave direct radiative effects of above-cloud aerosols over global oceans derived from 8 years of CALIOP and MODIS observations, Atmos. Chem. Phys., 16, 2877-2900, 10.5194/acp-16-2877-2016, 2016.

https://doi.org/10.5194/acp-2019-646
Preprint. Discussion started: 4 September 2019

Atmospheric Chemistry and Physics Discussions

Zhao, M. S., Heinsch, F. A., Nemani, R. R., and Running, S. W.: Improvements of the MODIS terrestrial gross and net primary production global data set, Remote Sens. Environ., 95, 164-176, 10.1016/j.rse.2004.12.011, 2005.

Zhao, M. S., and Running, S. W.: Drought-Induced Reduction in Global Terrestrial Net Primary Production from 2000 Through 2009, Science, 329, 940-943, 10.1126/science.1192666, 2010.

Zhao, Y., Zhang, J., and Nielsen, C. P.: The effects of energy paths and emission controls and standards on future trends in China's emissions of primary air pollutants, Atmos. Chem. Phys., 14, 8849-8868, 10.5194/acp-14-8849-2014, 2014.

Zou, Y., Wang, Y., Ke, Z., Tian, H., Yang, J., and Liu, Y.: Development of a REgion-Specific ecosystem feedback Fire (RESFire) model in the Community Earth System Model, J. Adv. Model Earth Sy., https://doi.org/10.1029/2018MS001368, 2019.

https://doi.org/10.5194/acp-2019-646
Preprint. Discussion started: 4 September 2019

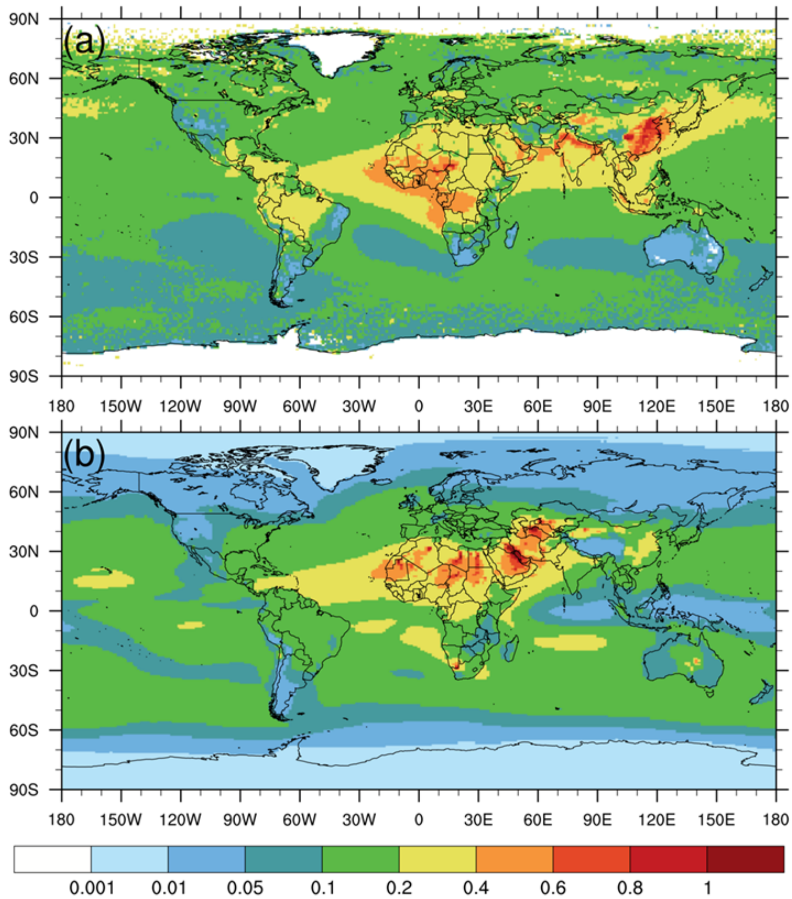

Figure 1: Comparison of annual averaged column AOD at 550 nm from (a) MODIS aboard the Aqua satellite (2003-2010); (b) CAM5 simulation averaged from 2001 to 2010.

https://doi.org/10.5194/acp-2019-646
Preprint. Discussion started: 4 September 2019

Atmospheric Chemistry and Physics
Discussions

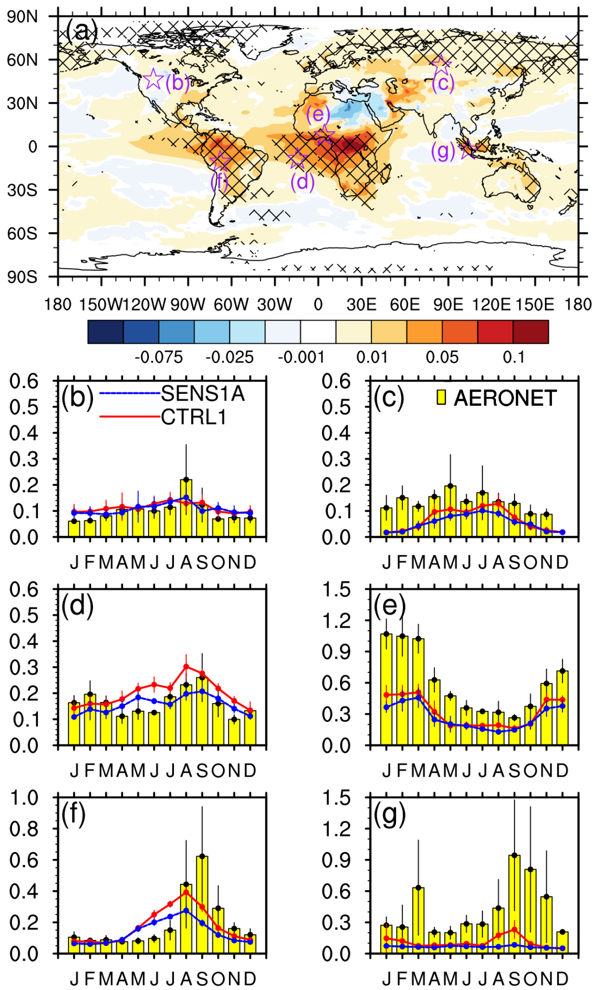

Figure 2: CESM-RESFire simulation of (a) annual averaged fire contributed AOD at 550 nm (shading) in the present-day scenario (CTRL1-SENS1A). The stars denote the AERONET site location and the net meshes denote the 0.05 significance level of the two-tailed Student's t-test; (b) comparison with AERONET in situ monthly AOT observations at 550 nm in Missoula (114.1°W, 46.9°N) during the 2000s. The error bars denote ±1 standard deviations of interannual variations in the simulations and observations, respectively.; (c) same as (b) but in Tomsk (85.1°E, 56.5°N); (d) same as (b) but in Ascension island (14.4°W, 8.0°S); (e) same as (b) but in Ilorin (4.3°E, 8.3°N); (f) same as (b) but in Rio Branco (67.9°W, 10.0°S); (g) same as (b) but in Jambi (103.6°E, 1.6°S).

https://doi.org/10.5194/acp-2019-646
Preprint. Discussion started: 4 September 2019

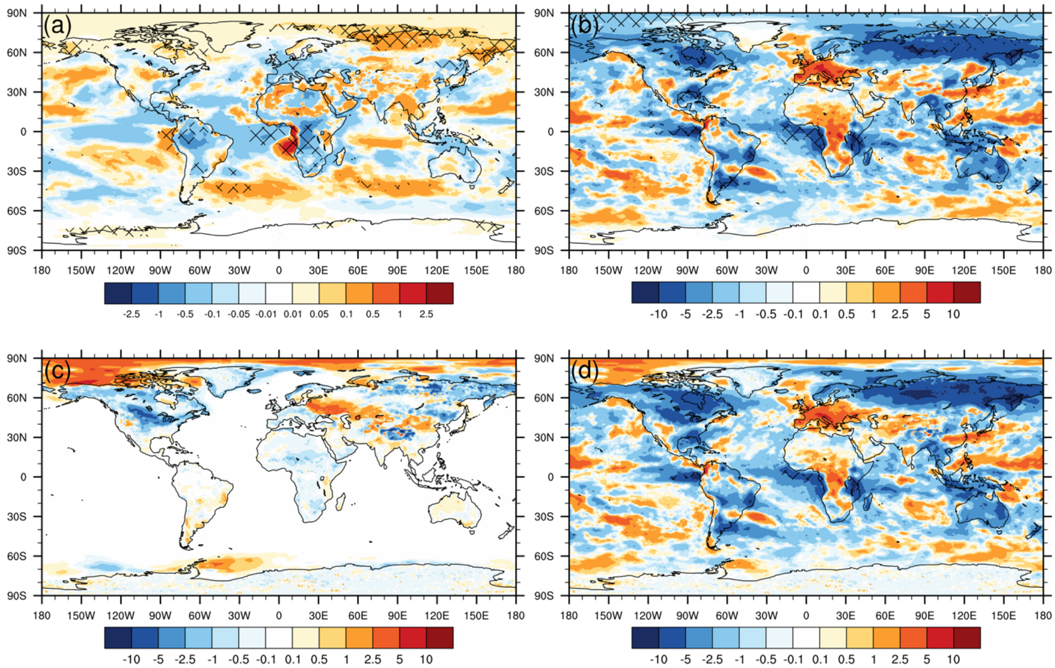

Figure 3: Present-day simulation of fire contributed annual averaged radiative effects through (a) aerosol-radiation interactions (RE_{ari}, W m^{-2}); (b) aerosol-cloud interactions (RE_{aci}, W m^{-2}); (c) fire aerosol-induced surface albedo change (RE_{sac}, W m^{-2}); (d) fire aerosol-related net radiative effects (RE_{aer}, W m^{-2}). The net meshes denote the 0.05 significance level.

https://doi.org/10.5194/acp-2019-646
Preprint. Discussion started: 4 September 2019

Atmospheric Chemistry and Physics Discussions

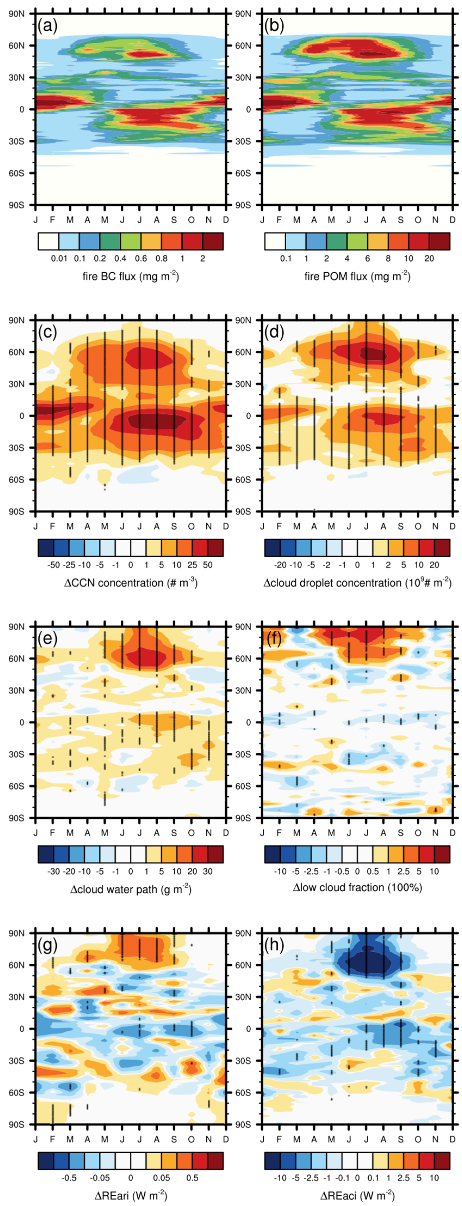

Figure 4: Present-day simulation of zonal averaged time-latitude cross sections of (a) monthly BC fire emission fluxes (mg m^{-2}) in CTRL1; (b) monthly POM fire emission fluxes (mg m^{-2}) in CTRL1; (c) fire-induced low-level (averaged below 800 hPa) cloud condensation nuclei (CCN, # m^{-3}) concentration changes (CTRL1-SENS1A); (d) vertically-integrated cloud droplet number concentration (CDNUMC, 10^{9}# m^{-3}) changes (CTRL1-SENS1A); (e) cloud water path (CWP, g m^{-2}) changes (CTRL1-SENS1A); (f) low cloud cover fraction (100%) changes (CTRL1-SENS1A); (g) radiative effect changes (CTRL1-SENS1A) by fire aerosol-radiation interactions (RE$_{ari}$, W m^{-2}); (h) radiative effect changes (CTRL1-SENS1A) by fire aerosol-cloud interactions (RE$_{aci}$, W m^{-2}). The dots in (c)-(h) denote the 0.05 significance level.

https://doi.org/10.5194/acp-2019-646
Preprint. Discussion started: 4 September 2019

Atmospheric Chemistry and Physics
Discussions

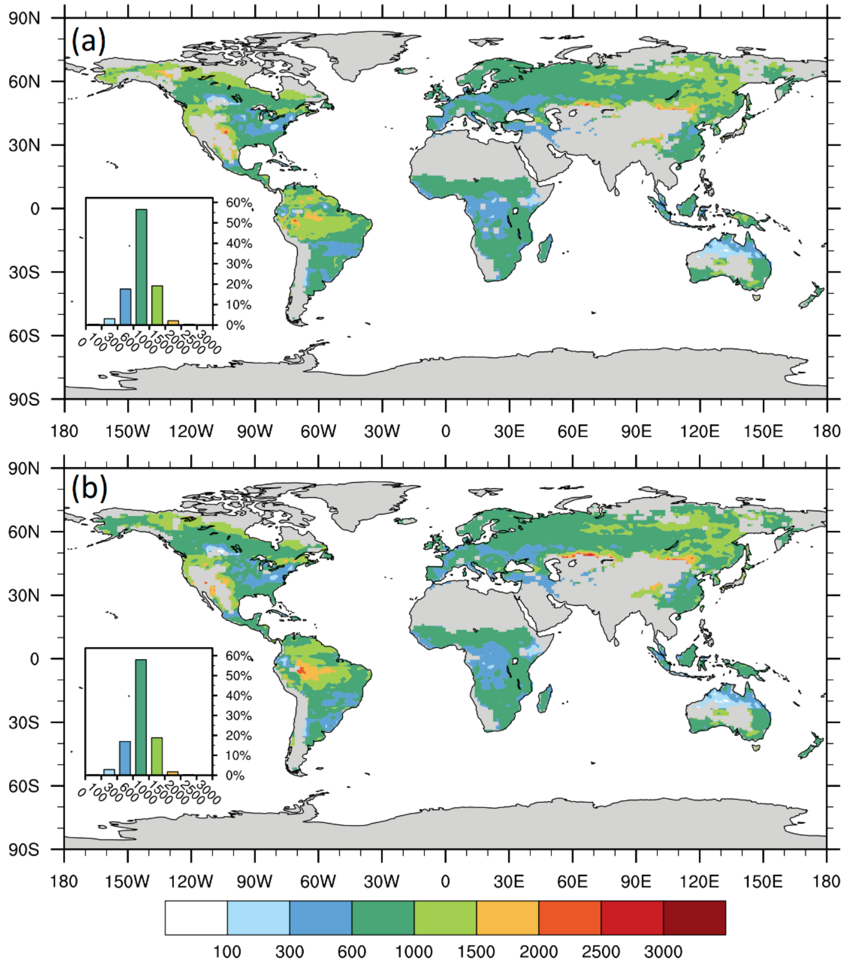

Figure 5: Comparison of CESM-RESFire simulated annual median injection heights (m) of fire plumes in the (a) present-day (CTRL1) and (b) RCP4.5 (CTRL2) scenarios. The inlets show statistical distributions of all plume injection heights in model grid cells of each scenario.

https://doi.org/10.5194/acp-2019-646
Preprint. Discussion started: 4 September 2019

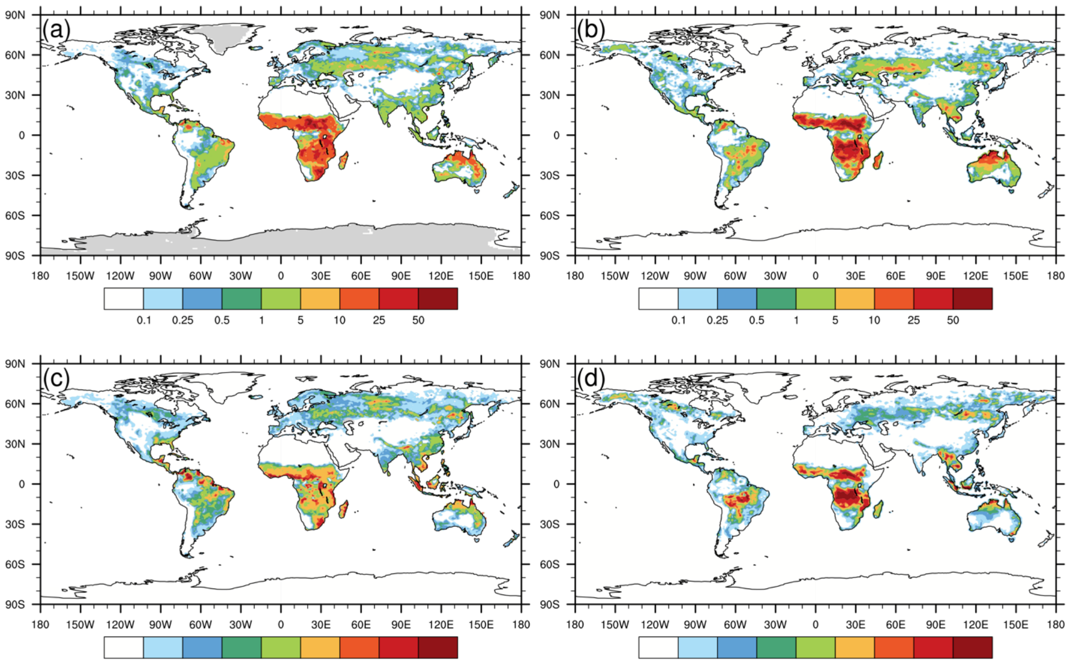

Figure 6: Comparison of CESM-RESFire simulations and GFED4.1s data. (a) ensemble averaged annual burned area (%) simulation; (b) 10-year averaged (2001-2010) annual burned area (%) based on the GFED4.1s data; (c) ensemble averaged annual fire carbon emission (gC m^{-2} yr^{-1}) simulation; (d) 10-year averaged (2001-2010) annual fire carbon emission (gC m^{-2} yr^{-1}) based on the GFED4.1s data.

https://doi.org/10.5194/acp-2019-646
Preprint. Discussion started: 4 September 2019

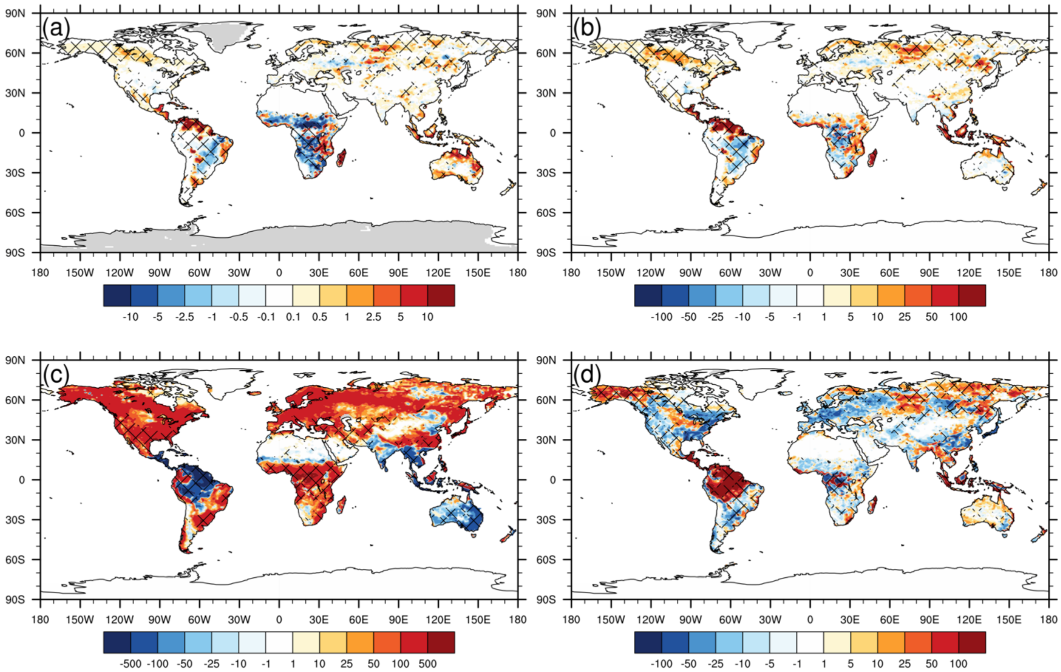

Figure 7: CESM-RESFire simulated changes between the RCP4.5 future scenario and the present-day scenario (CTRL2-CTRL1) in (a) annual burned areas (%); (b) annual averaged fire carbon emissions (gC m^{-2} yr^{-1}); (c) annual averaged GPP (gC m^{-2} yr^{-1}); (d) annual averaged NEE (gC m^{-2} yr^{-1}). The net meshes denote the 0.05 significance level.

https://doi.org/10.5194/acp-2019-646
Preprint. Discussion started: 4 September 2019

Atmospheric Chemistry and Physics Discussions
Open Access

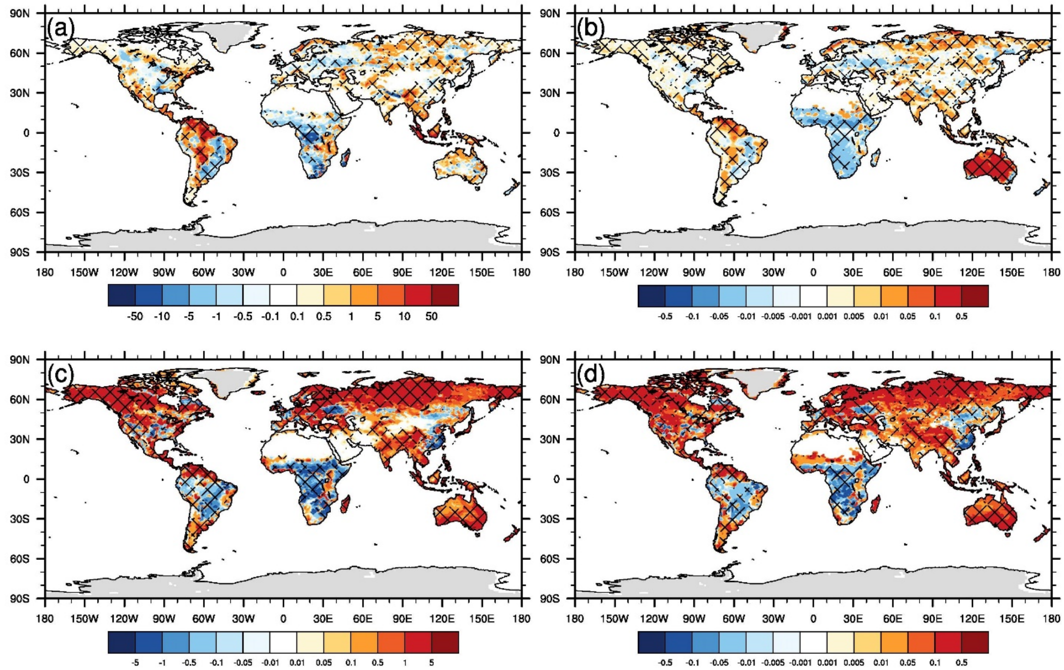

Figure 8: CESM-RESFire simulated changes in fire-related variables between the RCP4.5 future scenario and the present-day scenario (CTRL2-CTRL1). (a) changes in annual total fire ignition (NFIRE, 1E-3 count km^{-2} yr^{-1}); (b) changes in annual averaged fire combustion factors (FCF, unitless); (c) changes in annual averaged fire spread rates (FSR_DW, cm s^{-1}); (d) changes in annual averaged fire spread factors (FSF, unitless). The net meshes denote the 0.05 significance level.

https://doi.org/10.5194/acp-2019-646
Preprint. Discussion started: 4 September 2019

Atmospheric Chemistry and Physics
Discussions

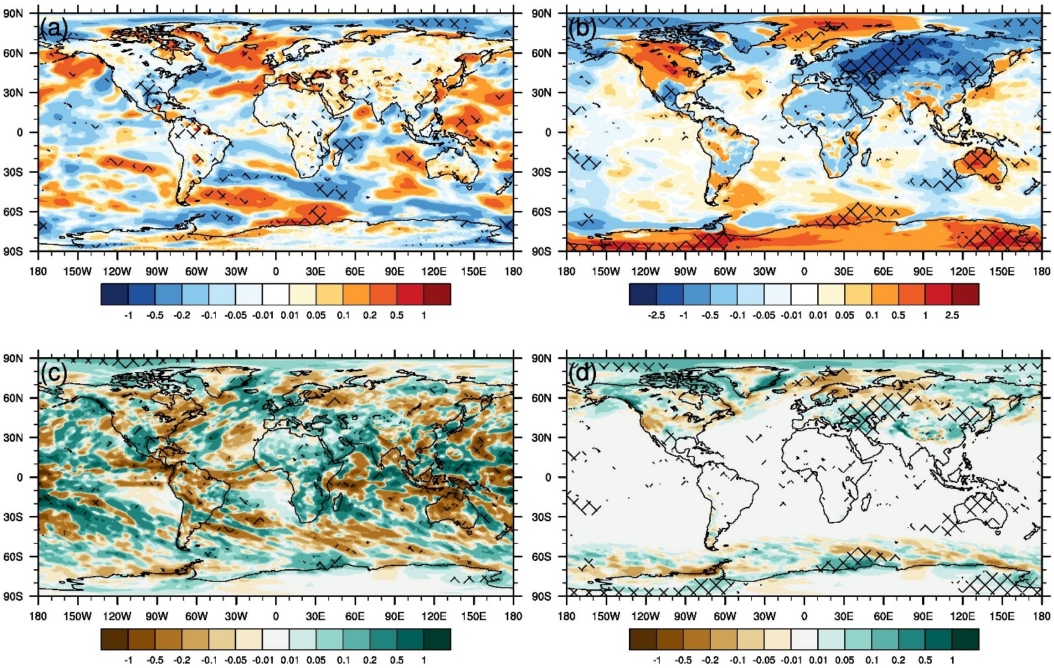

Figure 9: CESM-RESFire simulated changes in fire weather variables between the RCP4.5 future scenario and the present-day scenario (CTRL2-CTRL1). (a) changes in surface wind speed (m s^{-1}); (b) changes in surface temperature (K); (c) changes in rain precipitation (mm day^{-1}); (d) changes in snow precipitation (mm day^{-1}). The net meshes denote the 0.05 significance level.

https://doi.org/10.5194/acp-2019-646
Preprint. Discussion started: 4 September 2019

Atmospheric Chemistry and Physics
Discussions

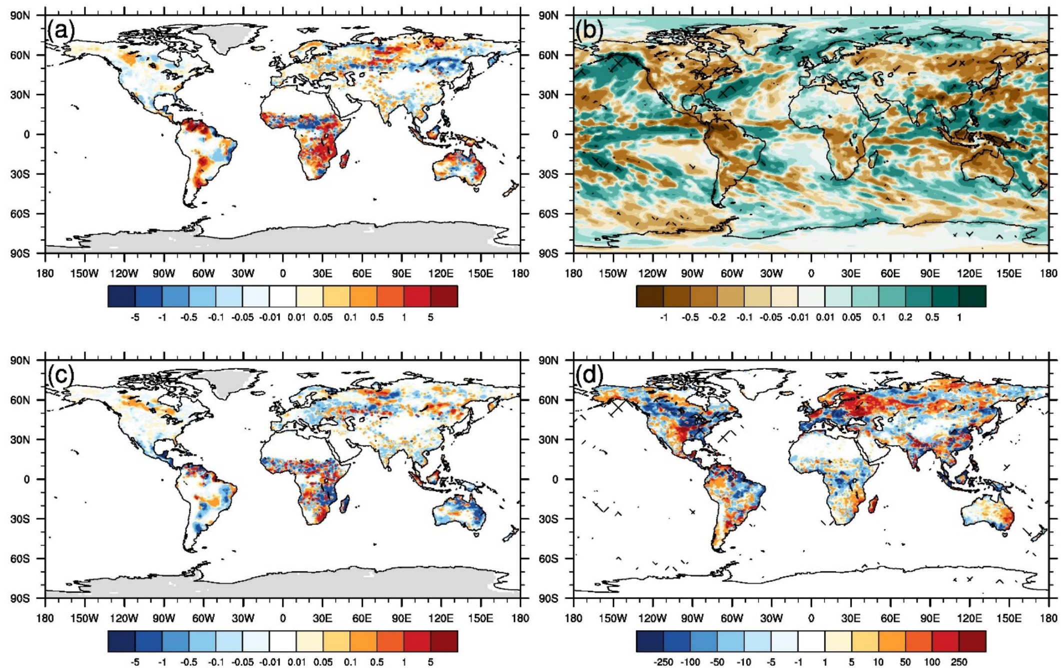

Figure 10: Comparison of climate-fire-ecosystem interactions in CESM-RESFire sensitivity experiments in the RCP4.5 future scenario. (a) differences of annual total burned areas (%) between fire emission sensitivity experiments (CTRL2-SENS2A); (b) same as (a) but for differences of precipitation rates (mm day^{-1}); (c) differences of annual total burned areas (%) between fire-induced land cover change sensitivity experiments (SENS2A-SENS2B); (d) same as (c) but for differences of annual averaged fuel loads (gC m^{-2}). The net meshes denote the 0.05 significance level.

https://doi.org/10.5194/acp-2019-646
Preprint. Discussion started: 4 September 2019

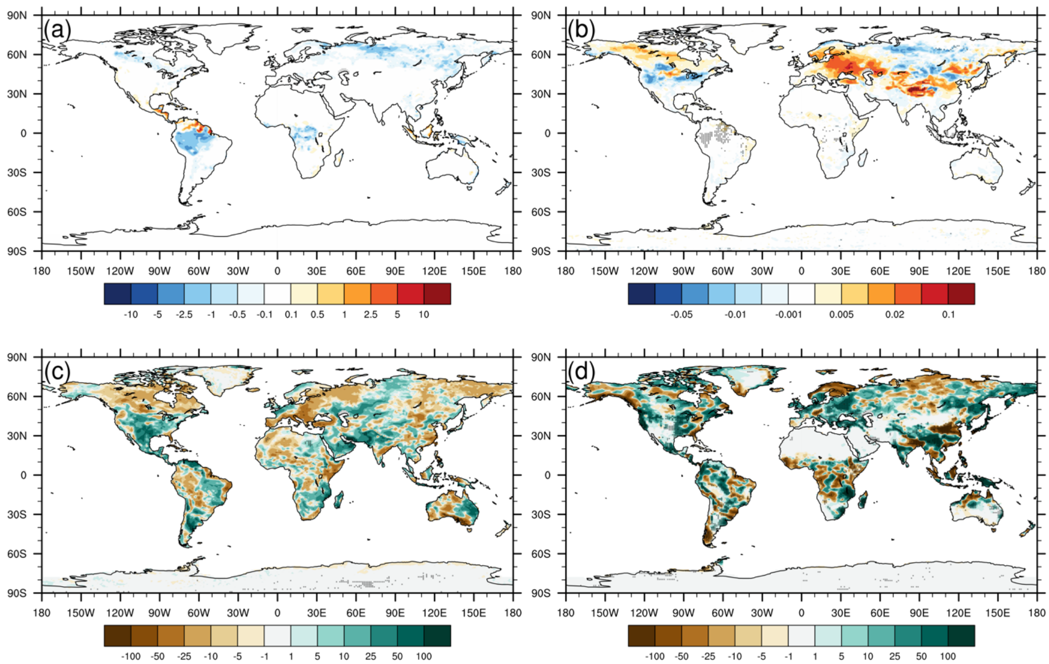

Figure 11: CESM-RESFire simulation of fire-related biophysical effects in the RCP4.5 future scenario. (a) differences of annual averaged fractional tree coverage (%) between fire-induced LCC sensitivity experiments (SENS2A-SENS2B); (b) same as (a) but for differences of surface albedo (proportion) in early spring (January-April); (c) same as (a) but for differences of evapotranspiration (mm yr^{-1}); (d) same as (a) but for differences of total runoff (mm yr^{-1}). The net meshes denote the 0.05 significance level.

https://doi.org/10.5194/acp-2019-646
Preprint. Discussion started: 4 September 2019

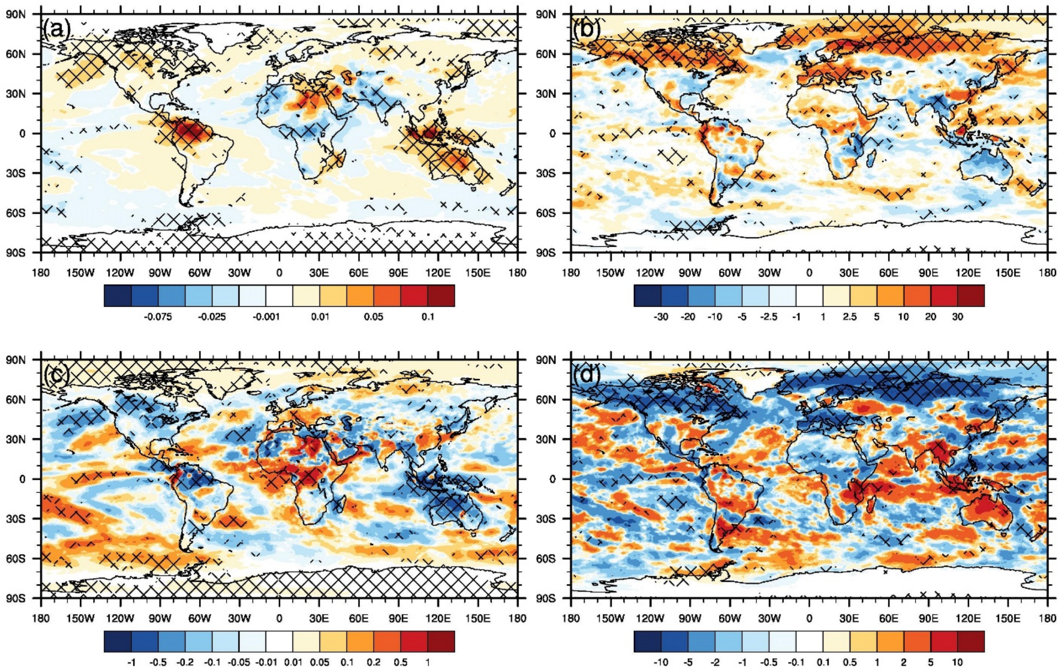

Figure 12: CESM-RESFire simulated changes of fire aerosol-related climate variables between the RCP4.5 future scenario (CTRL2-SENS2A) and the present-day scenario (CTRL1-SENS1A). (a) changes in annual averaged column AOD at 550 nm (unitless); (b) changes in CWP (g m^{-2}); (c) changes in RE_{ari} (W m^{-2}); (d) changes in RE_{aci} (W m^{-2}). The net meshes denote the 0.05 significance level.

https://doi.org/10.5194/acp-2019-646
Preprint. Discussion started: 4 September 2019

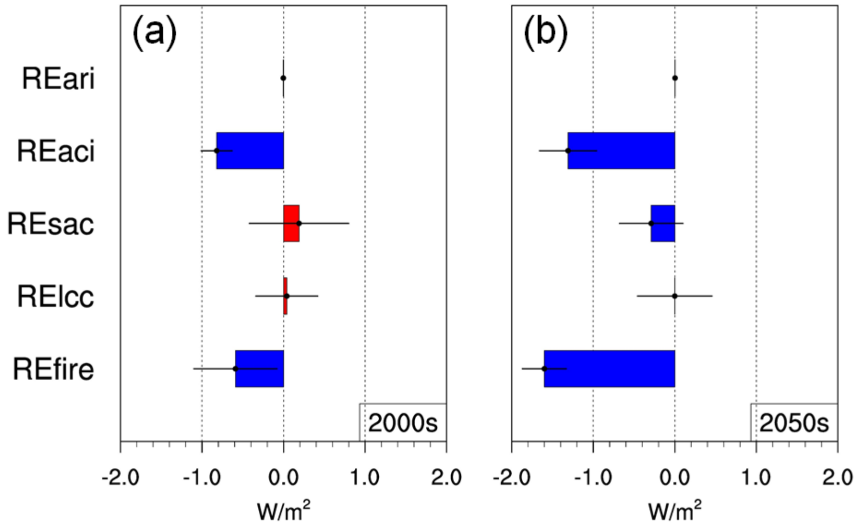

Figure 13: Comparison of CESM-RESFire simulated fire radiative effects (W m^{-2}) in (a) the present-day scenario and (b) the RCP4.5 future scenario. The error bars denote standard deviations of interannual variations during each 10-year simulation period.

https://doi.org/10.5194/acp-2019-646
Preprint. Discussion started: 4 September 2019

Atmospheric Chemistry and Physics
Discussions

868 **Table 1: Fire sensitivity simulation experiments for the present-day and RCP4.5 future scenarios**

Scenario	Present-day (2000)			Future (RCP4.5)		
Name	CTRL1	SENS1A	SENS1B	CTRL2	SENS2A	SENS2B
Time	2001-2010	2001-2010	2001-2010	2051-2060	2051-2060	2051-2060
Atmosphere	CAM5	CAM5	CAM5	CAM5	CAM5	CAM5
Land	CLM4.5	CLM4.5	CLM4.5	CLM4.5	CLM4.5	CLM4.5
Ocean	Climatology	Climatology	Climatology	RCP4.5 data	RCP4.5 data	RCP4.5 data
Sea ice	Climatology	Climatology	Climatology	RCP4.5 data	RCP4.5 data	RCP4.5 data
Non-fire emissions	IPCC AR5 emission data	IPCC AR5 emission data	IPCC AR5 emission data	RCP4.5 data	RCP4.5 data	RCP4.5 data
Fire emissions	Online fire aerosols with plume rise	—	—	Online fire aerosols with plume rise	—	—
Land cover	Fire disturbance on present-day conditions	Fire disturbance on present-day conditions	Fixed present-day conditions in 2000	Fire disturbance on RCP4.5 conditions	Fire disturbance on RCP4.5 conditions	Fixed RCP4.5 conditions in 2050

869

870

https://doi.org/10.5194/acp-2019-646
Preprint. Discussion started: 4 September 2019

Atmospheric Chemistry and Physics Discussions

Table 2: Comparison of fire-related radiative effects in the present-day (CTRL1-SENS1A) and RCP4.5 future (CTRL2-SENS2A) scenarios based on this work and previous studies

Unit: W m^{-2}	This work		Jiang et al. (2016)	Ward et al. (2012)	
Time	2000s	2050s	2000s	2000s (CLM3/GFEDv2)	2100s (CCSM/ECHAM)
RE_{ari}	-0.003±0.013*	0.003±0.033	0.16±0.01	0.10/0.13	0.12/0.25
RE_{aci}	-0.82±0.19	-1.31±0.35	-0.70±0.05	-1.00/-1.64	-1.42/-1.74
RE_{sac}	0.19±0.61	-0.29±0.39	0.03±0.10	0.00/0.01	0.00/0.00
RE_{aer}	-0.64±0.48	-1.59±0.33	-0.55±0.07	-0.90/-1.50	-1.30/-1.49
RE_{lcc}	0.04±0.38	-0.006±0.457	—	-0.20/-0.11	-0.23/-0.29
RE_{fire}	-0.59±0.51	-1.60±0.27	-0.55±0.07	-0.55**/—	-0.83/-0.87**

*: the numbers after ± denote standard deviations of interannual variations;

**: the net radiative forcing includes other effects such as GHGs and climate-BGC feedback;

https://doi.org/10.5194/acp-2019-646
Preprint. Discussion started: 4 September 2019

Atmospheric Chemistry and Physics Discussions
Open Access
EGU

Table 3. Comparison of fire and carbon budget variables between CESM-RESFire simulations and previous studies and benchmarks

Variables	Time Period	This work		CLM-LL2013 (Li et al., 2014)	Benchmark	Sources
Models		RESFire-CRUNCEP	RESFire-CAM5c	CLM4.5-DATM		
Burned area (Mha yr^{-1})	1997-2004	508 ± 15	472 ± 14	322	510 ± 27	GFED4.1s (Giglio et al., 2013; Randerson et al., 2012)
Fire carbon emissions (Pg C yr^{-1})	1997-2004	2.3 ± 0.2	2.6 ± 0.1	2.1	2.2 ± 0.4	GFED4.1s (van der Werf et al., 2017)
NEE (Pg C yr^{-1})	1990s	-2.6 ± 0.6	-2.0 ± 1.3	-0.8	-1.1 ± 0.9 -2.0 ± 0.8	IPCC AR5 (Ciais et al., 2013) 10 models average (Piao et al., 2013)
GPP (Pg C yr^{-1})	2000-2004	142 ± 2	142 ± 1	130	133 ± 15	10 models average (Piao et al., 2013)
NPP (Pg C yr^{-1})	2000-2004	62 ± 1	63 ± 0.7	54	54	Zhao and Running (2010)

Table 4. Comparison of carbon budget variables between the CRUNCEP data atmosphere driven fire simulations based on CESM-RESFire and CLM-LL2013

Variables		CESM-RESFire			CLM-LL2013 (Li et al., 2014)	
Unit: Pg C yr^{-1}	ΔFire	Fire on	Fire off	ΔFire	Fire on	Fire off
NEE	1.58	-2.67	-4.25	1.0	-0.1	-1.1
C_{fe}	2.08	2.08	0.0	1.9	1.9	0.0
-NEP+C_{lh}	-0.5	-4.75	-4.25	-0.9	-2.0	-1.1
NEP	0.5	4.8	4.3	0.8	3.0	2.3
NPP	0.4	61.7	61.3	-1.9	49.6	51.6
Rh	-0.1	56.9	57.0	-2.7	46.6	49.3
GPP	-0.1	142.3	142.4	-5.0	118.9	123.9
Ra	-0.5	80.6	81.1	-3.1	69.3	72.4
C_{lh}	0.0	0.05	0.05	-0.1	1.0	1.1

https://doi.org/10.5194/acp-2019-646
Preprint. Discussion started: 4 September 2019

885 **Table 5. Comparison of carbon budget variables between CESM-RESFire sensitivity experiments and previous studies**

Variables	This work						Kloster et al. (2010) Kloster et al. (2012)	
Time (scenario)	2000s (CTRL1)	2050s (CTRL2)	2000s (SENS1A)	2050s (SENS2A)	2000s (SENS1B)	2050s (SENS2B)	2000s	2050s
Burned area (Mha yr^{-1})	464±19	551±16 (↑19%)*	437±17 (↓6%)**	535±19 (↓3%)	458±18 (↓1%)	545±18 (↓1%)	176-330	–
Fire carbon emissions (Pg C yr^{-1})	2.5±0.1	5.0±0.3 (↑100%)	–	–	–	–	2.0-2.4	2.7/ 3.4
GPP (Pg C yr^{-1})	141±1.2	146±1.1 (↑4%)	143±1.0 (↑1%)	149±1.3 (↑2%)	142±1.5 (↑1%)	150±1.3 (↑3%)	–	–
NEP (Pg C yr^{-1})	1.4±0.04	1.5±0.04 (↑7%)	1.4±0.04 (→0%)	1.6±0.04 (↑7%)	1.4±0.02 (→0%)	1.6±0.05 (↑7%)	–	–
NEE (Pg C yr^{-1})	1.2±0.03	1.6±0.05 (↑33%)	1.2±0.02 (→0%)	1.6±0.05 (→0%)	1.2±0.02 (→0%)	1.6±0.05 (→0%)	–	–

886 *: percentage numbers in the parentheses under CTRL2 denote relative changes comparing with the CTRL1
887 scenario.
888 **: percentage numbers in the parentheses under SENSx (x=1 or 2) denote relative changes comparing with the
889 corresponding CTRLx (x=1 or 2) scenarios.